The influence of a dynamic solar shape on tests of gravitational theory using observations of Mercury missions

Rens van der Zwaard

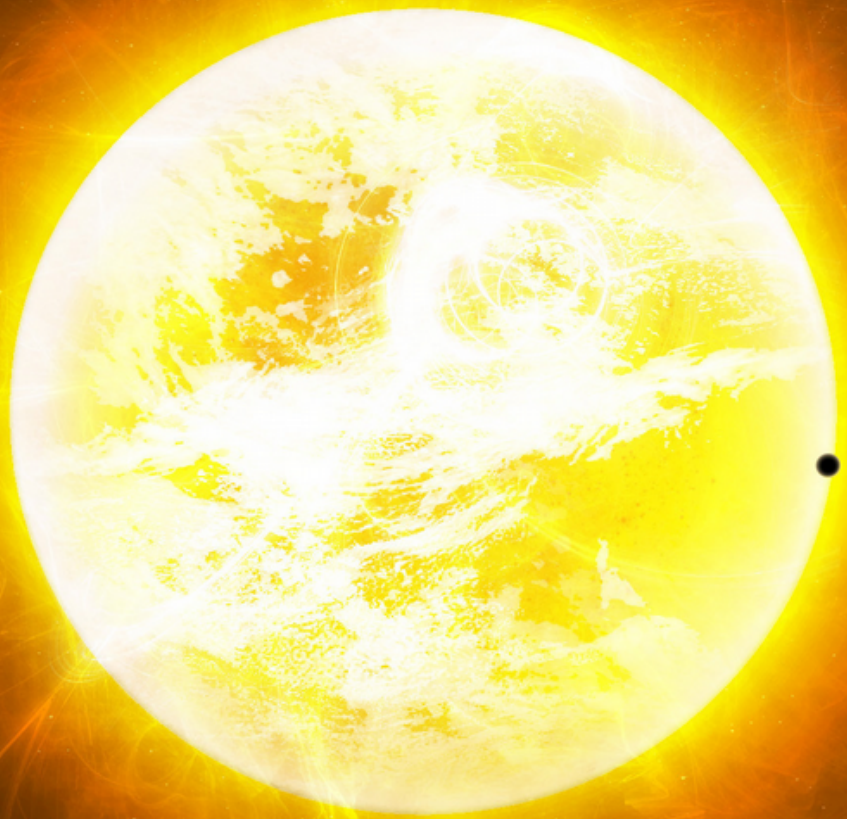

Technische Universiteit Delft

TU Delft

The influence of a dynamic solar shape on tests of gravitational theory using observations of Mercury missions

by

Rens van der Zwaard

to obtain the degree of Master of Science
at the Delft University of Technology,

Student number:	4290690	
Project duration:	February 2020 – 12 November 2020	
Thesis committee:	dr. ir. W. van der Wal	committee chair
	dr. ir. D. Dirkx	supervisor
	dr. A. Cervone	external examinator
	ir. M. Fayolle-Chambe	additional examinator

An electronic version of this thesis is available at `http://repository.tudelft.nl/`.

TU Delft

Abstract

Tests of General Relativity are often done in the Solar System by using tracking data from interplanetary space missions, to measure the perturbation on the orbits of the planets that is predicted by General Relativity. The next best opportunity for such a test is the BepiColombo spacecraft by the European Space Agency, which will arrive at Mercury in late 2025.

However, a very similar perturbation is also produced by the gravitational oblateness of the Sun through the zonal coefficient $J_{2\odot}$. The exact value of this coefficient has been hard to determine despite centuries of observations of the solar shape, and besides the accuracy of the tracking data it is the main source of uncertainty for the tests of gravitational theory. Recent publications in heliophysics suggest that higher order effects might also be of relevant influence too, such as coefficient $J_{2\odot}$ being dynamic along the solar cycle, or the fourth zonal coefficient $J_{4\odot}$.

This thesis project attempts to bring together two fields of research: the field that tries to test General Relativity (GR) in the Solar System, and the field of heliophysics that tries to unravel the structure of the Sun. The orbit of Mercury, as well as the observations of BepiColombo and it predecessor MESSENGER, are simulated in a virtual reality where settings of the solar shape are varied. Relevant parameters to tests of gravity are then estimated using a least-squares algorithm and their error is analysed.

It is found that the amplitude of a periodic component of the solar oblateness can be found with an uncertainty of 0.02% of the value of $J_{2\odot}$. It is also found that if a periodic component exists with an amplitude higher than 1%, it can lead to errors in the experiments of GR to the point that results oppose the theory of General Relativity. Expected values for $J_{4\odot}$ from heliophysics currently do not influence the orbit of Mercury by a measurable amount.

Based on this work, it is recommended to those in the field who test General Relativity using data from BepiColombo, to take this effect into consideration to prevent getting results in their experiments that can lead physicists in the wrong direction concerning the development of gravitational theory.

Preface

The adventure of being a student in Delft must come to an end. It has brought me so many great things in seven years, I would need a thesis report by itself to describe it all.

This thesis project started out of a general interest in relativity and gravity as a whole, without much prior knowledge of it at all. The fascination has only grown ever since, and with great interest I have read about the history and current state of gravitational physics. I was more than happy to add this little piece of work to a very large field of research, which most certainly still has an exciting future ahead of itself. I hope my findings do not cause too much chaos for the scientists who devote so much energy into figuring out the universe.

I want to thank Dominic for providing me with the freedom at the start of this thesis to figure out everything on my own, and of course the fruitful discussions during meetings. Even though we have met only physically once or twice in this entire thesis, your virtual support every week kept me motivated to work hard on this project.

Furthermore, I want to thank everyone who helped me stay in good spirits over the course of this thesis project. Without that, it would definitely have been impossible to finish such a large project during a pandemic.

Rens

Contents

1 Introduction 1

2 Journal article 5

3 Conclusions and Recommendations 21
3.1 Conclusions. . . . 21
3.2 Recommendations . . . 22
3.3 Testing General Relativity in the Solar System: a short outlook . . . 23

A Acceleration Models 25
A.1 Lense-Thirring acceleration correction . . . 25
A.2 Time-variable gravitational parameter . . . 26
A.3 Strong Equivalence Principle Violation . . . 26
A.4 Relativistic correction due to PPN parameters α_1 and α_2 . . . 29
A.5 Time variable gravitational moments . . . 30
A.6 Excluded accelerations . . . 30

B Observation construction 33
B.1 MESSENGER and BepiColombo tracking characteristics . . . 34
B.2 Orbiter error with respect to Mercury . . . 34
B.3 Simulated error construction . . . 36
B.4 Validity of simulated errors . . . 36

C Verification 39
C.1 Numerical integrator and propagator . . . 39
C.2 Acceleration partial derivatives . . . 42
C.3 Consider Covariance . . . 43

D Validation 45
D.1 Genova et al. 2018. . . . 46
D.2 Schettino 2015 . . . 47
D.3 Imperi 2018 . . . 48

Bibliography 51

Nomenclature

Abbreviations

ABM12	Adams-Bashford-Moulton integrator of order 12
ABM8	Adams-Bashford-Moulton integrator of order 8
EEP	Einstein Equivalence Principle
ESA	European Space Agency
IAA RAS	Institute of Applied Astronomy ofthe Russian Academy of Sciences
IMCCE	Institute for Celestial Mechanics and Computation of Ephemerides
JAXA	Japanese Aerospace Exploration Agency
JPL	Jet Propulsion Laboratory
LLI	Local Lorentz Invariance
MESSENGER	Mercury Surface, Space Environment, Geochemistry and Ranging
MOND	Modified Newtonian Dynamics
MORE	Mercury Orbiter Radioscience Experiment
PPN	Parameterised Post-Newtonian
RK4	Runge-Kutta integrator of order 4
RK7(8)	Runge-Kutta-Fehlberg integrator of order 7-(8)
SEP	Strong Equivalence Principle
SPE angle	Sun-Probe-Earth angle
SSB	Solar System Barycentre

Symbols

$\boldsymbol{\rho}$	Residuals
$\boldsymbol{a}$	acceleration vector
$\boldsymbol{C}$	Consider parameter covariance matrix
$\boldsymbol{c}$	Consider parameter vector
$\boldsymbol{H_c}$	Partial derivatives of observations w.r.t. the consider parameters $\boldsymbol{c}$
$\boldsymbol{H_x}$	Partial derivatives of observations w.r.t. the state vector $\boldsymbol{x}$
$\boldsymbol{P}$	covariance matrix
$\boldsymbol{p}$	Estimatable parameter vector
$\boldsymbol{P}^C$	Consider covariance matrix
$\boldsymbol{P}_0$	Apriori covariance matrix

$\boldsymbol{r}$	position vector
$\boldsymbol{S}_\odot$	Solar angular momentum vector
$\boldsymbol{v}$	velocity vector
$\boldsymbol{W}$	Observation weight matrix
$\boldsymbol{x}$	State vector $\left[\boldsymbol{y}, \boldsymbol{p}\right]^T$
$\boldsymbol{y}$	Body state $[\boldsymbol{r}, \boldsymbol{v}]^T$
η	Nordtvedt parameter
$\frac{\dot{GM}}{GM}$	time variation of gravitational parameter
$\gamma, \beta, \xi, \alpha_1, \alpha_2, \alpha_3, \zeta_1, \zeta_2, \zeta_3, \zeta_4$	Parameters of the PPN framework
$\mathbf{I}$	Idendity matrix
μ, GM	gravitational parameter
c	speed of light in vacuum
G	gravitational constant
$J_{d\odot}$	Solar Spherical Harmonics zonal coefficient of degree d
M	mass
r	distance (norm of position vector $\boldsymbol{r}$)
$S_\odot$	Solar angular momentum magnitude

1

Introduction

In 1859 French astronomer Urbain Le Verrier discovered that the perihelion of Mercury shifts over time by an amount which could not be accounted for only by calculating the perturbations caused by the planets [34]. Le Verrier did not get the right value at that point but presently it is known that the anomalous advance is 43 arcseconds per century. Many proposals were made to solve the problem by suggesting undiscovered planets or a large solar gravitational oblateness [51], but any evidence was never found.

In the 19$^{\text{th}}$ century, laws of electromagnetism were developed, which lead to the formulation of the theory of Special Relativity in 1905 [11]. This theory was not compatible with Newton's laws of gravity, which lead Einstein to develop a new, relativistic, theory of gravity. In 1915 the result was published: the theory of General Relativity [12]. To support the theory, it was calculated that the anomalous advance could exactly be explained with General Relativity, which predicted the first post-Newtonian acceleration correction exerted by the Sun to be exactly 43 arcseconds per century.

Ever since, the experiment of Mercury's perihelion has become famous. Due to better observations over the course of the 20$^{\text{th}}$ century, the anomalous precession could be measured with increasing precision. Even smaller effects could now be measured as well, and the question was raised: what perturbations contribute to end up with this measured advance of Mercury's perihelion? The perturbations caused by the planets could be calculated with sufficiently high accuracy, but one other perturbation was hard to predict: the advance due to the solar gravitational oblateness of the Sun around its equator, i.e. the zonal harmonic of degree 2. This effect is dictated by zonal coefficient $J_{2\odot}$. Measuring this parameter is difficult, because among other reasons the interior (i.e. mass distribution) is unknown, the surface rotation is not the same for all latitudes and the visual shape of the Sun is hard to observe due to magnetic surface activity [38, 48]. Due to uncertainty about the value of $J_{2\odot}$, it could not be calculated with confidence how much of the 43 arcseconds was caused by the solar oblateness and how much had to be caused by something else, presumably a post-Newtonian term of relativistic gravitational theory.

It is for that reason, that scientists in the 1960's briefly started to doubt General Relativity. A considerably higher value for the solar oblateness was measured, which resulted in the statement that the perturbation predicted by General Relativity was off by 8% [9]. This resulted in a lot of controversy, and after years of discussion the observations were rejected by the community [48]. The search for the right value for $J_{2\odot}$ continued, but there were still large discrepancies between measurements. A sufficiently accurate input for the perihelion advance caused by solar oblateness could not be found by observing the Sun, hampering the proof of the effect predicted by General Relativity.

Experiments to prove General Relativity using planetary orbits have been ongoing in the meantime. While it is commonly accepted in the scientific community as the leading theory of gravity and it has survived countless experiments, many questions remain unanswered. For example, General Relativity is not compatible with quantum physics, and the field of particle physics has been searching for a way to explain gravitational interactions at a microscopical level [35]. In addition, many questions are still open about the evolution of the universe in the field of cosmology [51, 56]. Therefore, one hundred years after its formulation, there still is a demand for more accurate tests of General Relativity.

The problem of the solar oblateness was however still present. In the 21$^{\text{st}}$ century, experiments of General Relativity were developed which took into account hundreds of thousands of observations of planet positions over decades, and constraints on both parameters of General Relativity and $J_{2\odot}$ could be determined along-

side each other through estimation, eliminating the need for a good value of $J_{2\odot}$ from solar observations. The estimation is however held back by high correlation between the parameters that dictate the relativistic perturbation and $J_{2\odot}$, because they both produce the same effect: an advance in the perihelion of planets. Nevertheless, the results of such experiments are often presented very confidently: for $J_{2\odot}$, reported uncertainties of experiments got to a 1σ uncertainty of 1% recently [17]. It is however not uncommon that estimates of the value of $J_{2\odot}$ vary between experiments within 10% (see [48] or figure 1 of the upcoming journal paper for recent results). Therefore, it can be questioned whether estimates of $J_{2\odot}$, and in extension the parameters of General Relativity, are published with overconfident uncertainty.

In heliophysics, observing the Sun and its shape has continued nevertheless, because about the interior and dynamics of the Sun there are still many questions to be answered. In the last two decades, it has more than once been suggested based on oblateness observations that the solar oblateness might not be a constant value, but varies over time along with the solar magnetic activity cycle (e.g. [3, 28, 46, 48]), although the theory is also contested [32]. It was calculated that a dynamic value for $J_{2\odot}$ could cause perturbations in the rate that the advance of Mercury's perihelion occurred in the order of 1% [58], the same magnitude as the claimed uncertainty of recent estimations of the parameter. Furthermore, theories and measurements considering the fourth order zonal coefficient $J_{4\odot}$ have come up [1, 3, 37, 38, 48], which could also influence the orbit of Mercury at a measurable amount if large enough. The impact of these recent suggestions about the gravity perturbations caused by the solar shape have never been included or investigated in the experiments made to prove General Relativity. Because estimations with planetary observations proved to be more effective in estimating $J_{2\odot}$, the solar physics side of the story behind the solar oblateness seems to be a bit separated from the gravity experiments, at least when compared to the past.

Currently speaking, the next best chance to do such a test is currently on its way to Mercury: the BepiColombo mission, a collaboration between the European Space Agency (ESA) and the Japanese Aerospace Exploration Agency (JAXA), which will arrive in December 2025. One of the two spacecraft that will orbit Mercury has dedicated hardware, the Mercury Orbiter Radioscience Experiment (MORE, [20]), on board to improve the constraints on the parameters that are associated with the perturbation caused by General Relativity. The aim is to improve the uncertainty with two orders of magnitude [26, 39, 49].

The solar gravitational oblateness could stand in the way of achieving this goal. In the new regime of accuracy that BepiColombo will provide, what kind of phenomena will be encountered for the solar oblateness, as suggested in the past 2 decades in heliophysics? In this work, it is attempted to address this question. The aim is to research what kind of scenarios for the solar shape are presented by literature in heliophysics, and see what the impact would be on the experiments of General Relativity using BepiColombo data. In general, the hypothesis that is to be proven right or wrong in this work is:

> **The time variable gravitational oblateness or higher order zonal effects of the Sun can have a relevant effect on the tests of general relativity that will be done using BepiColombo data, and it should be taken into account in experiments of gravity that use BepiColombo data.**

The following research questions have been formulated that need to be answered to achieve this goal: **Using combined tracking data of the MESSENGER and BepiColombo missions in a parameter estimation algorithm,**

1. **to what accuracy can parameters of General Relativity and the solar quadrupole moment $J_{2\odot}$ be determined?**
   In the past, parameters were estimated with MESSENGER data [21, 43], and predictions have been made by simulating BepiColombo data [4, 26, 27, 39, 49], but the two data sets have never been combined before. It is of interest to know if this long-term combined data set has considerable advantages for long-term effects. Furthermore, this will set a baseline of what the algorithm made in this project is capable of when not including any higher order effects in the solar shape.

2. **what dynamic values for $J_{2\odot}$ can be detected?**
   Periodic variations of a variety of magnitudes are suggested by publications in heliophysics, what theorethical values could be detected with this data set?

3. **can higher order effects due to other zonal coefficients $J_{n\odot}$ be detected?**
   Again, a variety of values is suggested in literature, which ones can be detected?

4. **if higher order effects do exist but are not considered in gravitational experiments, what will be the impact in the estimation of relativistic parameters?**
   It can be imagined that a mismodelling of the solar oblateness can lead to large errors in gravitational experiments. Just like 1960's, this could lead to controversy if measurements start to conflict with General Relativity.

This report is structured as follows. The thesis work has been written down in the shape of a scientific journal article, which will be presented next in the second chapter of this report. In chapter 3 extensive conclusions and recommendations will be given for the thesis. To support the methods developed during this thesis, which are only briefly explained in the journal article, Appendix A will elaborate further upon the acceleration models used and appendix B will give a detailed description of how observations are simulated. Finally, verification and validation of the software will be elaborated upon in appendix C and D, respectively.

For those interested, the software used for this thesis project is made available. All simulations are performed in TUDAT ([10], `https://tudat.tudelft.nl/`)*, for the libraries the most recent version was taken on February 2020. Post-processing is done in Python 3.6. All written code is uploaded to the following github repositories:*

- *The main applications, custom functions, inputs and post-processing procedures:* `https://github.com/RensZ/thesis2`
- *Changes made in the acceleration and estimation models in the* /tudatBundle/tudat/Tudat/ *folder:* `https://github.com/RensZ/Tudat`

It is a large piece of code made to run a large variety of simulations, I would be happy to help you along or answer any questions that you may have regarding the code, just shoot me a message: rensvanderzwaard@gmail.com.

The influence of a dynamic solar shape on tests of gravitational theory using observations of Mercury missions

Rens van der Zwaard

Delft University of Technology, Kluyverweg 1, 2629HS Delft, the Netherlands
rensvanderzwaard@gmail.com

October 28, 2020

Abstract

When the BepiColombo spacecraft arrives at Mercury in late 2025, it will be able to measure the orbit of the planet with unprecedented accuracy, allowing for more accurate measurements of the perihelion advance of the planet as predicted by the theory of General Relativity (GR). A similar effect is produced by the gravitational oblateness of the Sun through the zonal coefficient $J_{2\odot}$. The shape of the Sun has been hard to determine despite centuries of observations, causing high uncertainties in the experiments of GR. Recent publications in heliophysics suggest that $J_{2\odot}$ is not a constant but a dynamic value that varies with solar magnetic activity, and that the next zonal effect $J_{4\odot}$ could also be of relevant influence. The aim of this paper is to analyse what the effect is of suggested higher-order effects of the solar shape on experiments of the perihelion advance of Mercury as predicted by GR. The orbit of Mercury and observations of the MESSENGER and BepiColombo spacecraft are simulated, and parameters corresponding to gravitational theory as well as the oblateness $J_{2\odot}$ including a time-variable component are estimated using a least-squares approach. The result of the estimation is that the amplitude of a periodic component can be found with an uncertainty of $3.7 \cdot 10^{-11}$, equal to 0.017% the value of $J_{2\odot}$. It is also found that if a periodic component exists with an amplitude higher than 1% the value of $J_{2\odot}$ and it is not considered, it can lead to errors in the experiments of GR using BepiColombo data to the point that results falsely confirm or oppose the theory of General Relativity. Expected values for $J_{4\odot}$ from heliophysics currently do not influence the orbit of Mercury by a measurable amount.

1. Introduction

The Solar System has always been a suitable laboratory for testing gravitational theory. An often-used test is the secular precession of Mercury's perihelion, of which it was discovered in the 19^{th} century that it could not be explained just by using Newtonian gravity and third-body interactions of other planets (Le Verrier, 1859). Albert Einstein used the observed precession of Mercury's perihelion as a key test to confirm his Theory of General Relativity (GR, Einstein, 1916). Ever since, experiments on gravitational interactions have only confirmed General Relativity with increasing accuracy. General Relativity is however not able to provide all the answers about gravitational interactions yet in fundamental physics, especially on the scales of quantum mechanics or cosmology (Shapiro, 1999; Mattingly, 2005; Will, 2014). Therefore, more than one hundred years after the theory was introduced, testing General Relativity and its underlying principles is still a hot topic. Finding absolute correctness or microscopic deviations of General Relativity is of high relevance in the search for a universal theory in fundamental physics. The current state, future outlook and relevance of experiments on General Relativity is provided in great detail by (Will, 2014). In this paper the relativistic influence on the secular precession of Mercury's orbit will be the focus.

The commonly used tool for experiments on gravity is the Parameterised Post-Newtonian (PPN) framework (Will & Nordtvedt, 1972), which uses ten parameters $(\gamma, \beta, \xi, \alpha_1, \alpha_2, \alpha_3, \zeta_1, \zeta_2, \zeta_3, \zeta_4)$. In General Relativity these parameters take on the values $\gamma, \beta = 1$ and $\xi, \alpha_1, \alpha_2, \alpha_3, \zeta_1, \zeta_2, \zeta_3, \zeta_4 = 0$, however many alternative theories of gravity have been formulated which predict different values for the parameters (see Will, 2014). The

determination of the PPN parameters through experiment is a method to test which gravitational theories are viable.

The orbit of Mercury is a test subject for such an experiment. The first order post-Newtonian perturbation is the perihelion advance, which can be expressed as a function of the PPN parameters. Per orbit of Mercury around the Sun, the precession is equal to $\Delta\tilde{\omega}$ (Will, 2014, eq. 66):

$$\Delta\tilde{\omega} = \frac{6\pi}{p}\left[\frac{1}{3}(m_\odot + m_M)(2 + 2\gamma - \beta) + \frac{1}{6}(2\alpha_1 - \alpha_2 + \alpha_3 + 2\zeta_2)\left(\frac{m_\odot m_M}{m_\odot + m_M}\right)\right] \quad (1)$$

where $m_\odot$ and m_M are the masses of the Sun and Mercury and p is the semi-latus rectum of the orbit of Mercury around the Sun. With accurate observations of the orbit of Mercury the values of the PPN parameters can be constrained. However, the second order zonal effect of the Sun, caused by the mass bulge at the equator, produces a similar effect which has to be considered (Park et al., 2017, eq. 3):

$$\Delta\tilde{\omega} = \frac{6\pi}{p}\left(\frac{J_{2\odot}R^2}{2p}\right)\left(1 - \frac{3}{2}\sin^2 i\right) \quad (2)$$

$J_{2\odot}$ is the normalised zonal coefficient of degree 2 of the Sun, R is the mean radius of the Sun and i is the inclination of the orbit of Mercury with respect to the solar equator. A major source of uncertainty in experiments of the PPN parameters is caused by the uncertainty of $J_{2\odot}$.

Attempts to determine the shape of the Sun date back to the 19$^{\text{th}}$ century. The determination of the visual oblateness (the visual radius difference between equator and poles) has turned out to be challenging, because among other reasons the interior (i.e. mass distribution) is unknown, the surface rotation is not the same for all latitudes and the visual shape of the Sun is hard to observe due to magnetic surface activity. A comprehensive overview of experiments and their challenges is provided by Rozelot and Damiani (2011), see also discussions by (Damiani et al., 2011; Meftah et al., 2016). Zonal coefficient $J_{2\odot}$, which influences bodies orbiting the Sun, appears to not relate directly to its visual shape and its rotation rate (Rozelot & Damiani, 2011; Will, 1981), and therefore the field of heliophysics has had trouble to come up with constraints on $J_{2\odot}$ that are useful as input for tests on gravitational physics. It is for that reason that in experiments that use planetary orbits, parameter $J_{2\odot}$ is usually estimated alongside the PPN parameters. This limits the precision of the experiment, as γ, β and $J_{2\odot}$ are all linearly proportional to the precession rate of Mercury's perihelion. γ can be distinguished through other experiments due to its effect on the propagation of light (see Bertotti et al., 2003), but for β or $J_{2\odot}$ no other experiment is available. This causes a high correlation between β and $J_{2\odot}$ in their estimation. Because of this, the uncertainty of the solar oblateness can be considered a bottleneck for testing gravitational theory.

To illustrate the challenge of determining $J_{2\odot}$, figure 1 shows selected attempts to determine the value of $J_{2\odot}$ both by estimation using planetary orbits and by the field of heliophysics. It can be observed that

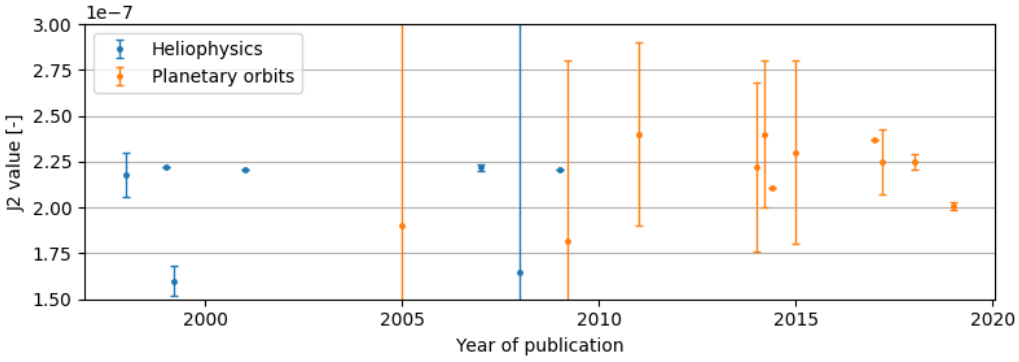

Figure 1: *Selected attempts to determine $J_{2\odot}$ over the last 25 years. Errorbars indicate the 2σ uncertainty, corresponding to a 95% confidence level. Where no error bars are drawn, uncertainties were not provided. All entries in this plot are provided at the end of the paper in table 5.*

uncertainties are often quite optimistic and results are not consistent with each other, presumably due to the correlation of $J_{2\odot}$ and other parameters, or other assumptions that are made in the determination of the parameter and its uncertainty.

To complicate matters further, it is suggested that higher order zonal effects such as $J_{4\odot}$ could also be of significant value to affect planetary orbits at a measurable level (Antia et al., 2007; Rozelot & Damiani, 2011). In addition, recent publications in heliophysics state that the visual solar oblateness varies along the 11-year solar activity cycle, and a similar periodic variation in the value of $J_{2\odot}$ is suggested (Rozelot et al., 2009; Irbah et al., 2019), although this theory has also been contested (Kuhn et al., 2012). The effect that a dynamic value of $J_{2\odot}$ would have on the planetary orbits has been calculated by Xu et al., 2017 and the importance of considering it in gravitational experiments has been mentioned by Pireaux & Rozelot, 2003, in both cases it is concluded that the dynamic effect can have relevant influence on tests of General Relativity. Nevertheless, a dynamic oblateness has so far never been considered in publications about solar system ephemerides or experiments of gravitational physics.

The aim of this study is to bridge the gap between heliophysics and gravitational physics, by investigating the different configurations that are suggested for the solar gravity field. The central question of this study is: with the observational capabilities of Mercury that are expected in the foreseeable future, can the various hypotheses about the solar gravity field be confirmed or rejected, and do they have a relevant influence on tests of General Relativity? If certain hypotheses can be confirmed or rejected, it is of great value to both fields to refine their theoretical models further.

The best test subject for such a study is the orbit of Mercury. To date, the best experiments use data from the MESSENGER spacecraft by NASA which orbited Mercury from 2011 until 2015, see e.g. (Verma et al., 2014; Park et al., 2017; Genova et al., 2018). The best next opportunity will be the BepiColombo mission by ESA, which is currently in cruise phase and will be inserted into Mercury orbit in 2025 for a nominal mission of one year. It will provide tracking data with unprecedented accuracy with its dedicated instrument: the Mercury Orbiter Radioscience Experiment (MORE, Genova et al., 2008), due to its dual-frequency tracking in the X and Ka bands. Simulations of relativity experiments using simulated BepiColombo tracking data show 1 to 2 orders of magnitude improvements for constraints on β (Milani et al., 2002; Ashby et al., 2007; Iess et al., 2009; Schettino et al., 2015; Imperi, Iess, & Mariani, 2018). Neither the experiments with MESSENGER data or the simulations of experiments with BepiColombo data have ever considered perturbations due to higher order effects due to the solar shape besides a constant $J_{2\odot}$. In this work, a similar experiment will be set up which will consider such higher order effects. Tracking data of both MESSENGER and BepiColombo will be simulated, resulting in one combined data set which will span 20 years, allowing to track the effect of small perturbations on the orbit of Mercury over the long term.

2. Method

At the top level our experiment is set up as follows. A virtual reality is created by integrating the orbit of Mercury from 2008 to 2028, with the acceleration model described in section 2.1 and all parameters set corresponding to the theory of General Relativity being correct. Using the numerically integrated position of Mercury in the virtual reality, range observations are simulated according to the methods described in section 2.2. The observations are used as input to estimate a set of parameters in a least-squares algorithm, which will be explained in section 2.3. The software used for simulation and estimation is the TU Delft Astrodynamics Toolbox (TUDAT, Dirkx et al., 2019).

2.1. Accelerations acting on Mercury

For the numerical integration of Mercury, an acceleration model is set up to take into account all perturbations that can produce an effect that is measurable using the MESSENGER and BepiColombo tracking data. In general these perturbations are: central gravity accelerations by celestial bodies in the Solar System, figure effects of the Sun, first-order post-Newtonian relativistic effects caused by the Sun and finally possible deviations of General Relativity.

The point mass accelerations are included of all relevant Solar System bodies which are the Sun, the 7 planets, the Moon and the 300 most influential asteroids. Positions of the bodies are obtained from ephemeris DE430 (Folkner et al., 2014) using SPICE.

For the accelerations due to figure effects of the Sun, dictated by normalised zonal coefficients $J_{2\odot}$ and $J_{4\odot}$, spherical harmonics are used (see e.g. Montenbruck & Gill, 2000). To model a time variable zonal coefficient, a

simple sine function is taken as a correction $c_{J_d}(t)$ that is added to the zonal coefficient:

$$c_{J_d}(t) = A_{J_{2\odot}} \sin\left(\frac{2\pi}{P}t + \varphi\right) \tag{3}$$

$A_{J_{2\odot}}$ is the amplitude of the periodic variation and will be included as a parameter in the estimation. Period P and phase φ are chosen such that the correction aligns with the solar activity cycle. In figure 2 the monthly smoothed sunspot number has been plotted, and the mission durations of MESSENGER and BepiColombo have been indicated on the x-axis. A period of 11 years is chosen with a phase tuned such that the correction reaches a minimum in December 2008 and December 2019. The sunspot number is commonly accepted as the measure for solar magnetic activity. Therefore it should be noted that, under the assumption that the variations in oblateness mainly depend on solar magnetic activity (as also shown in (Irbah et al., 2019)), a sinusoidal correction is only a first order approximation.

For the gravitational force exerted by the Sun the post-Newtonian relativistic acceleration is implemented according to equation 7.42 of (Will, 1981). The assumption is made that the mass of Mercury m_M is negligibly small to the mass of the Sun $m_\odot$. Furthermore, we only consider gravitational theories that comply with conservation laws for total momentum, meaning PPN parameters $\alpha_3, \zeta_1, \zeta_2, \zeta_3$ and ζ_4 are all zero, because theories that violate total momentum lack experimental evidence and are therefore unlikely candidates for describing gravitational interactions (Will, 2014). The resulting acceleration term for Mercury is the following:

$$\begin{aligned}\mathbf{a}_{\mathrm{PN}} = &\frac{Gm_\odot}{c^2 r^3}\left\{\left[2(\beta+\gamma)\frac{Gm_\odot}{r} - \gamma(\mathbf{v}\cdot\mathbf{v})\right.\right.\\ &+ (2+\alpha_1)\frac{Gm_M}{r} - \frac{1}{2}(6+\alpha_1+\alpha_2)\frac{m_M}{m_\odot}(\mathbf{v}\cdot\mathbf{v})\\ &\left.+ \frac{3}{2}(1+\alpha_2)\frac{m_M}{m_\odot}\left(\mathbf{v}\cdot\frac{\mathbf{r}}{r}\right)^2\right]\mathbf{r}\\ &\left.+ \left[2(1+\gamma) - \frac{m_M}{m_\odot}(2-\alpha_1+\alpha_2)\right](\mathbf{r}\cdot\mathbf{v})\mathbf{v}\right\}\end{aligned} \tag{4}$$

where $\mathbf{r}$ and $\mathbf{v}$ are the relative position and velocity vectors of Mercury with respect to the Sun, G is the universal gravitational constant and c is the speed of light in vacuum.

Furthermore, the angular momentum of the Sun $\mathbf{S}_\odot$ produces the perturbation known as the Lense-Thirring effect, which is included as follows (Petit & Luzum, 2010):

$$\mathbf{a}_{\mathrm{LT}} = (1+\gamma)\frac{Gm_\odot}{c^2 r^3}\left[\frac{3}{r^2}(\mathbf{r}\times\mathbf{v})(\mathbf{r}\cdot\mathbf{S}_\odot) + (\mathbf{v}\times\mathbf{S}_\odot)\right] \tag{5}$$

In addition, the Strong Equivalence Principle (SEP) is considered, of which the validity is an important building block of General Relativity. The SEP states that the inertial and gravitational masses are considered to be equal in any experiment in a gravity field, e.g. planets in the gravity field of the Sun, and that the self-gravitational energy Ω_i of the bodies themselves do not play a role (Kopeikin et al., 2011). To parameterise

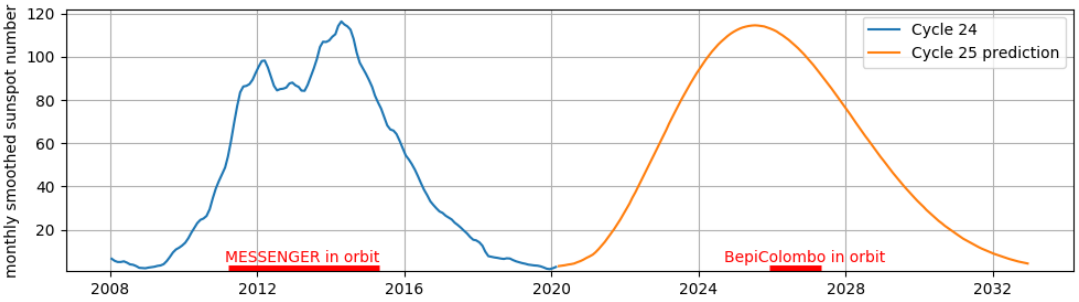

Figure 2: *Monthly smoothed sunspot numbers from January 2008 to August 2020 in blue (SILSO World Data Center, 2020) and the prediction of solar cycle 25 in orange (NOAA Space Weather Prediction Center, 2020), which expects the next solar maximum in July 2025 with an uncertainty of 8 months. The periods that MESSENGER and BepiColombo are in orbit around Mercury are indicated in red on the x-axis. The period indicated for BepiColombo is the nominal mission duration of 1 year.*

the SEP, the Nordtvedt parameter η is used which can be expressed as a function of PPN parameters (Will, 1981, sec. 8.1):

$$\eta = 4(\beta - 1) - (\gamma - 1) - \alpha_1 - \frac{2}{3}\alpha_2 \tag{6}$$

where it is again assumed that $\alpha_3, \zeta_1, \zeta_2, \zeta_3, \zeta_4 = 0$. If the SEP and therefore General Relativity is correct, $\eta = 0$. If the SEP is violated, η has a nonzero value. It was determined by (Milani et al., 2002; Genova et al., 2018) that for Mercury the highest perturbation that is caused by a SEP violation, is the fact that the location of the Solar System Barycenter (SSB) changes when the SEP is violated. This means that the the position of the Sun with respect to the SSB has to be redefined:

$$\mathbf{r}_{\odot}^{SEP} = -\frac{1}{\mu_{\odot}\left(1 - \eta\frac{\Omega_{\odot}}{m_{\odot}c^2}\right)} \sum_{j \neq \odot} \left(1 - \eta\frac{\Omega_j}{m_j c^2}\right) \mu_j \mathbf{r}_j \tag{7}$$

which induces a change in the point-mass acceleration term exerted by the Sun on Mercury due to the change in the distance between the bodies.

Finally, the variation of the gravitational parameter $\mu_{\odot} = Gm_{\odot}$ is considered. General Relativity predicts that the gravitational constant G is constant across space and time, but other theories have suggested that G may vary with the evolution of the universe (Will, 2014; Uzan, 2011). In addition, the solar mass $m_{\odot}$ changes over time due to the radiative output of the Sun and solar winds. The combination of the variation of these two parameters is expressed as:

$$\frac{\dot{\mu}_{\odot}}{\mu_{\odot}} = \frac{G\dot{m}_{\odot}}{Gm_{\odot}} = \frac{\dot{G}}{G} + \frac{\dot{m}_{\odot}}{m_{\odot}} \tag{8}$$

In this study a constant time variation $G\dot{m}_{\odot}/Gm_{\odot}$ is assumed.

2.2. Simulated observations

To perform the estimation of parameters of interest, observations of the position of planet Mercury over time are required. In reality, these observations are obtained from spacecraft tracking data, which provide a range measurement between a ground station on Earth and the spacecraft. To obtain a measurement of the range to the centre of gravity of the planet, the distance of the spacecraft with respect to Mercury has to be considered as well. The sum of these two distances is the distance from an Earth ground station to Mercury, which are the observations used as input for gravity experiments:

$$d_{\mathrm{E-M}} = d_{\mathrm{E-S/C}} + d_{\mathrm{S/C-M}} \tag{9}$$

where subscript E stands for Earth, M stands for Mercury and S/C stands for spacecraft. Similarly, both measurements contain errors. To obtain the error level of the observation of Mercury with respect to Earth, the root mean square is taken of the error levels of the individual terms:

$$\sigma^2_{d_{\mathrm{E-M}}} = \sigma^2_{d_{\mathrm{E-S/C}}} + \sigma^2_{d_{\mathrm{S/C-M}}} \tag{10}$$

The errors of the simulated observations are an important input for our experiment, they dictate the uncertainty at which parameters can be estimated. Therefore it is explained below how errors $\sigma^2_{d_{\mathrm{E-S/C}}}$ and $\sigma^2_{d_{\mathrm{S/C-M}}}$ are simulated to match as closely as possible to the errors that are encountered during the space missions.

As range observations from Earth to the spacecraft ($d_{\mathrm{E-S/C}}$) two-way range data is simulated for which the following inputs were taken. For MESSENGER, the range accuracy depends on the Sun-Probe-Earth (SPE) angle. The errors increase considerably at lower angles due to interference caused by solar plasma (Genova et al., 2018). A two-way noise level of 0.5 to 3.0 meters is used, depending linearly on the SPE angle with minimum noise at 180° and maximum noise at 35°. Observations are not simulated when the SPE angle is below 35° as its errors are too high to be of use in this experiment. BepiColombo range data does not suffer from interference due to solar plasma due to its multi-frequency radio links and therefore the noise level is constant and data at any SPE angle can be used (Iess et al., 2009). The target two-way noise level for BepiColombo is 20 to 30 centimetres (Iess & Boscagli, 2001), first reports from the cruise phase of BepiColombo even give centimetre-level errors (Cappuccio et al., 2020). A conservative range noise level of 30 centimetres is chosen for range simulations in this work.

The distance from the spacecraft to Mercury and its error ($\sigma^2_{d_{\mathrm{S/C-M}}}$) are usually determined through orbit determination of the spacecraft with respect to Mercury. For this purpose range-rate (doppler) measurements are especially useful. Because of constraints in computational power during this project, the MESSENGER and BepiColombo spacecraft could not be numerically integrated alongside Mercury. The consequence is that orbit determination cannot be performed and the distance including error could not be obtained in

the traditional way. Instead, it is chosen to artificially generate errors which are added to the observations. To achieve a realistic error, it was analysed what typical spacecraft position errors are by simulating various benchmark tracking arcs along the mission duration and performing orbit determination. It was found that the position errors of the spacecraft with respect to Mercury are largely based on two factors: the geometry between the spacecraft and Earth in the Solar System (which varies over months) and the true anomaly of the spacecraft in its orbit around Mercury (which varies over minutes). Through interpolation, set up to depend on these two factors, distance errors $\sigma^2_{d_{\mathrm{S/C-M}}}$ are generated from typical error levels that were found in the analysis of the benchmark tracking arcs. The results for the obtained error levels match with those reported for both missions (Genova et al., 2018; Verma et al., 2014; Alessi et al., 2012)

Having obtained the error level $\sigma^2_{d_{\mathrm{E-M}}}$, a random Gaussian error sample is generated and added to the observation. The tracking schedules (frequency of observations) are taken similarly to (Mazarico et al., 2014) for MESSENGER and (Cicalo et al., 2016) for BepiColombo. For both missions, one range observation is simulated as well as for each Mercury flyby that was performed during the cruise phase.

2.3. Parameter estimation

The goal of the estimation is to determine with what precision the initial state of Mercury and parameters $\gamma, \beta, \eta, G\dot{m}_\odot/Gm_\odot, J_{2\odot}, J_{4\odot}, A_{J_{2\odot}}$ can be constrained using the observations. The estimation is performed using a batch non-linear least-squares algorithm, as described in (Montenbruck & Gill, 2000, chapter 7 and 8). Before starting the least-squares algorithm, model observations are generated by integrating the orbit of Mercury with a perturbed initial state, such that the observations differ from the "real" observations simulated using the virtual reality. The least-squares algorithm calculates a correction on the initial state and parameters according to the following equation:

$$\Delta \boldsymbol{x}_0^{lsq} = \left(\boldsymbol{P}_0^{-1} + \boldsymbol{H}^T \boldsymbol{W} \boldsymbol{H}_x\right)^{-1} \left(\boldsymbol{P}_0^{-1} \Delta \boldsymbol{x}_0^{apr} + \boldsymbol{H}_x^T \boldsymbol{W} \Delta \boldsymbol{z}\right) \tag{11}$$

where $\Delta \boldsymbol{x}_0^{lsq}$ is the update on the parameter vector $\boldsymbol{x}$ which includes the initial state of Mercury and the estimatable parameters, $\boldsymbol{P}_0$ is the apriori covariance matrix, $\boldsymbol{H}_x$ is a matrix with partial derivatives of the observations with respect to the parameters and $\Delta \boldsymbol{z}$ is the difference between the real observations and modelled observations. $\boldsymbol{W}$ is the observation weight matrix, which represents the measurement error covariance, where the final error level is used as input (see section 2.2). Independent observations are assumed, i.e. $\boldsymbol{W}$ is a diagonal matrix.

2.3.1 Apriori information

To take past results of gravitational experiments into account, the estimation is provided with apriori information about the uncertainties on the parameters through apriori covariance matrix $\boldsymbol{P}_0$. The current best results for parameters are given in table 1. From the table, the top entry is taken for each parameter. Even though this is not always the best result published, apriori values are chosen to depend as much as possible on experiments that are not similar to ours (specifically, using past results based on MESSENGER data is avoided).

For PPN parameter γ the present known accuracy is $2.3 \cdot 10^{-5}$ from the Cassini solar superior conjunction experiment (Bertotti et al., 2003). It is suggested that BepiColombo could carry out similar superior conjunction experiments during its mission (Imperi & Iess, 2017), of which it is expected that at maximum an uncertainty of $1.1 \cdot 10^{-6}$ can be attained for γ (Imperi et al., 2018), a factor 20 increase with respect to the Cassini experiment. For both the current known value and hypothetical value of the apriori uncertainty results will be presented in section 3.

For parameter $J_{2\odot}$, choosing a result from any particular previous experiment is not sensible, because many seem too optimistic as is evident from figure 1. A value of $2.25 \cdot 10^{-7}$ is chosen, which is about average of the recent results. A conservative apriori uncertainty of $1 \cdot 10^{-7}$ is taken.

2.3.2 Consider covariance analysis

Ideally, every single parameter that can influence the dynamics of Mercury is included in the least-squares estimation, because very few variables are truly constant with no uncertainty. Assuming certain parameters are constant with no uncertainty is an option, but it could cause overly optimistic results in the end for the parameters that are estimated. As a compromise, a consider covariance analysis is used in this study (Montenbruck & Gill, 2000, section 8.1.4). Use is made of consider parameters: parameters that are not included in the pa-

Table 1: *Results of parameters from recent experiments. 1σ values are given for uncertainties.*

parameter	result	method
γ	$1 + (2.1 \pm 2.3) \cdot 10^{-5}$	Cassini solar conjunction (Bertotti et al., 2003)
β	$1 + (1.2 \pm 1.1) \cdot 10^{-4}$	Lunar Laser Ranging (Williams et al., 2012)
	$1 + (-2.7 \pm 3.9) \cdot 10^{-5}$	MESSENGER tracking data (Park et al., 2017)
	$1 + (-1.6 \pm 1.8) \cdot 10^{-5}$	MESSENGER tracking data (Genova et al., 2018)
	$1 + (0 \pm 7) \cdot 10^{-5}$	INPOP13c (Fienga et al., 2015)
α_1	$(0.8 \pm 4) \cdot 10^{-6}$	Planetary perihelion precession (Iorio, 2014)
	$(-0.4 \pm 1.9) \cdot 10^{-5}$	Small-eccentricity binary pulsars (Shao & Wex, 2012)
α_2	$(0 \pm 8) \cdot 10^{-10}$	Millisecond pulsars (Shao et al., 2013)
	$(4 \pm 6) \cdot 10^{-6}$	Planetary perihelion precession (Iorio, 2014)
η	$(3.1 \pm 3.6) \cdot 10^{-4}$	INPOP17a & Lunar Laser Ranging (Viswanathan et al., 2018)
	$(-6.6 \pm 7.2) \cdot 10^{-5}$	MESSENGER tracking data (Genova et al., 2018)
$Gm_\odot$ $\left[\mathrm{m^3 s^{-2}}\right]$	$(132712440040.042 \pm 0.010) \cdot 10^9$	INPOP19a (Fienga et al., 2019)
$\mathbf{S}_\odot$ $\left[\mathrm{kgm^2 s^{-1}}\right]$	$(190 \pm 1.5) \cdot 10^{39}$	Helioseismology (Pijpers, 1998)
$\frac{\dot{Gm_\odot}}{Gm_\odot}$ $\left[\mathrm{year}^{-1}\right]$	$(0 \pm 7) \cdot 10^{-14}$	INPOP13c (Fienga et al., 2015)
	$(-6.3 \pm 2.2) \cdot 10^{-14}$	EPM2011 (Pitjeva & Pitjev, 2013)

rameter estimation, but of which the uncertainty is to be considered when computing the formal uncertainty of estimated parameters.

The parameter covariance matrix including consider covariance matrix is expressed as follows (Montenbruck & Gill, 2000, eq. 8.42):

$$\boldsymbol{P}^c = \boldsymbol{P} + \left(\boldsymbol{P}\boldsymbol{H}_x^T\boldsymbol{W}\right)\left(\boldsymbol{H}_c\boldsymbol{C}\boldsymbol{H}_c^T\right)\left(\boldsymbol{P}\boldsymbol{H}_x^T\boldsymbol{W}\right)^T \quad (12)$$

where $\boldsymbol{P}$ is the final covariance matrix of the least-squares algorithm, $\boldsymbol{H}_c$ is a matrix with linearised partial derivatives of the observations with respect to the consider parameters and $\boldsymbol{C}$ is the apriori covariance matrix of the consider parameters (independence of consider parameters is assumed, i.e. $\boldsymbol{C}$ is diagonal).

In this study, the following parameters are implemented as consider parameters:

- The gravitational parameter of the Sun $Gm_\odot$.
- PPN parameters α_1 and α_2.
- Solar angular momentum $\mathbf{S}_\odot$.
- The gravitational parameters of the 300 most influential asteroids (a good discussion on the perturbations and uncertainties caused by the asteroids is given in (Park et al., 2017)).

For the first three bullets the apriori knowledge (value and uncertainty) is taken from table 1, for the asteroids the apriori knowledge is taken from INPOP19a (Fienga et al., 2019).

These parameters are selected as consider parameters because they have a significant influence on the formal errors of the parameters that are of interest in this study. However, estimating these parameters themselves is not of interest and significantly increases computational effort.

2.3.3 Estimation output

The covariance matrix $\boldsymbol{P}^c$ of the estimated parameters is an important piece of output. The square root of the diagonal entries represent the formal errors of the parameters. The formal error of a parameter is a 1σ uncertainty and should be interpreted as the 1σ confidence that the least-squares algorithm has in the result of the parameter estimation.

The formal error does not necessarily have to be indicative of the true error of the estimation. Relatively high true errors compared to formal errors often occur when dynamical effects in the acceleration model are mismodelled (which usually also results in high observation residuals) or when the observation weight matrix $\boldsymbol{W}$ does not represent the real observation errors. When the model is correct and the estimation algorithm is successful, true and formal errors are usually of the same magnitude or the true errors are smaller. Because in this work a simulated reality is used where each estimated parameter is assigned a "true value", it is possible to calculate the true errors for our results by comparing the estimation output with the virtual reality. In parameter estimation problems with real satellite tracking data this will not be possible and high true errors compared to formal errors lead to wrong estimates of parameters and phenomena.

2.3.4 Nordtvedt constraint

The Nordtvedt constraint (eq. 6) is an extra piece of information that can help the estimation algorithm. In particular, exploiting this relation prevents high correlation between the PPN parameters with each other and other parameters in the estimation (Genova et al., 2018; Imperi et al., 2018). To implement this equation, parameter η is not estimated in the least-squares algorithm but is calculated through the Nordtvedt constraint. In the results in section 3 the formal error of η is calculated using the property that the variance of a linear equation of parameters is (Dekking et al., 2005):

$$\mathrm{Var}\left(\sum_{i=1}^{m} a_i X_i\right) = \sum_{i=1}^{m}\sum_{j=1}^{n} a_i a_j \,\mathrm{Cov}\left(X_i, X_j\right) \qquad (13)$$

The formal variance of η can be calculated by applying this property to the Nordtvedt constraint:

$$\begin{aligned}\mathrm{Var}\left(\eta\right) = \mathrm{Var}\left(\gamma\right) + 16\mathrm{Var}\left(\beta\right) + \mathrm{Var}\left(\alpha_1\right) + \frac{4}{9}\mathrm{Var}\left(\alpha_2\right) \\ - 8\mathrm{Cov}\left(\gamma,\beta\right) + 2\mathrm{Cov}\left(\gamma,\alpha_1\right) + \frac{4}{3}\mathrm{Cov}\left(\gamma,\alpha_2\right) \\ - 8\mathrm{Cov}\left(\beta,\alpha_1\right) - \frac{16}{3}\mathrm{Cov}\left(\beta,\alpha_2\right) + \frac{4}{3}\mathrm{Cov}\left(\alpha_1,\alpha_2\right)\end{aligned} \qquad (14)$$

However, the covariance terms with one or both of α_1 and α_2 (last 5 terms) are neglected, as these terms cannot be calculated from the estimation output if α_1 and α_2 are included as consider parameters (see next section). The consequence is that the formal error of the Nordtvedt parameter is a bit on the higher side in our results, as the largest neglected covariance term is the one between β and α_1. This covariance is positive which causes a negative term in equation 14, decreasing the variance of η.

3. Results

3.1. Validation

Prior to generating results, the software has been verified and validated. The numerical integration error of Mercury's orbit is approximately 1 centimetre after 20 years of integration, which is assumed to be sufficient considering the noise level of BepiColombo observations is a factor 30 higher. Validation has been done by comparing the simulation to selected publications for MESSENGER (Genova et al., 2018) and BepiColombo (Schettino et al., 2015; Imperi et al., 2018). When using the same inputs and acceleration models (as far as possible), the formal error of our estimation can be seen in table 2. Our reproduction of these publications give uncertainties within a factor 2 for all parameters when compared to the result from the publication itself. As there are many design choices to be made in the setup of such a simulation, and it is not unusual to see differences of a factor 2 or more between similar experiments, this reproduction is considered successful. This validation procedure shows that, despite the simplifications that had to be made in the simulation of observations, our setup serves as a valid method for simulating a gravity experiment of Mercury tracking data.

The simulations in the validation stage were performed with models and inputs matching those presented in the respective publications, to reproduce the results as closely as possible. Results presented in the remainder of this paper follow the methods presented in section 2. In case of the formal errors presented in tables 2 to 4, true errors are in the same order of magnitude as the formal errors, indicating a good fit for the estimation. Range residuals are in the order of hundreds of meters for the MESSENGER data, and in the order of decimetres for the BepiColombo measurements, which are the minimum achievable values considering the simulated errors (see section 2.2) and an indication of a good least-squares fit. The state errors of planet Mercury follow the same pattern, having a formal uncertainty in the order of decimetres when BepiColombo data is used.

3.2. Estimation with a static solar oblateness

Before going into results with higher-order effects of the solar shape, we first present the results of an estimation with settings that are conventional in comparable experiments previously reported in literature: a static parameter $J_{2_\odot}$ and no other perturbations of the Sun due to spherical harmonics. These settings are implemented both for the simulated reality and the estimation. Formal uncertainties of estimated parameters are reported in table 3. Results of the estimation are shown when only using either MESSENGER or BepiColombo data and also when using a combined data set.

Formal errors for PPN parameters γ and β and Nordtvedt parameter η are comparable to the estimation when only using BepiColombo data, indicating that the estimation does not benefit from the combined data approach. These three parameters all cause a perihelion shift in the orbit of Mercury. The short but accurate

data set of BepiColombo is well suited to detect this effect. Even though the cumulative perihelion advance rise when observing over the long term, the errors of the MESSENGER observations are too high to be able to provide a better estimate than just with the BepiColombo data on the short term.

The long-term data set does however have an advantage for estimating the time variable gravitational parameter $G\dot{m}_\odot/Gm_\odot$, as an improvement of one order of magnitude can be found with respect to the estimation that only uses BepiColombo tracking data. The effect caused by the time variable gravitational parameter is a weakening of gravitational interactions causing Mercury to slowly drift away from the Sun, which is different to the perihelion shift which only changes the orientation of the elliptical orbit compared to the Sun but does not change it. Using the combined data set helps to decorrelate these effects: correlation coefficients of $G\dot{m}_\odot/Gm_\odot$ with the other three parameters are around 0.1 compared to 0.5-0.6 in the case of only using BepiColombo data.

To show the potential of the suggested BepiColombo superior conjunction experiment (see section 2.3.1), results are also shown in table 3 when an improved apriori uncertainty of γ is used corresponding to the expected outcome of such an experiment: $\sigma_\gamma = 1.1 \cdot 10^{-6}$. The strength of the superior conjunction experiment is clear from the results: improvements of a factor two can be obtained for both β and $J_{2\odot}$. The formal uncertainty of γ from the parameter estimation with apriori $\sigma_\gamma = 2.3 \cdot 10^{-5}$ cannot beat the result of the superior conjunction experiment.

Table 2: *Formal uncertainties (1σ) reported by recent gravity experiments using tracking data of MESSENGER or simulated tracking data of BepiColombo, and a reproduction of the formal uncertainties (1σ) of the publications using our software and similar inputs, compared for validation purposes.*

	γ	β	η	$J_{2\odot}$	$\frac{G\dot{m}_\odot}{Gm_\odot}$ $[\mathrm{y}^{-1}]$
results from (Genova et al., 2018)	$2.3 \cdot 10^{-5}$	$1.8 \cdot 10^{-5}$	$7.2 \cdot 10^{-5}$	$2 \cdot 10^{-9}$	$1.5 \cdot 10^{-14}$
reproduction of (Genova et al., 2018)	$2.3 \cdot 10^{-5}$	$2.0 \cdot 10^{-5}$	$8.4 \cdot 10^{-5}$	$3.4 \cdot 10^{-9}$	$2.1 \cdot 10^{-14}$
results from (Schettino et al., 2015)	$8.9 \cdot 10^{-7}$	$3.8 \cdot 10^{-7}$	$2.0 \cdot 10^{-6}$	$3.7 \cdot 10^{-10}$	$2.0 \cdot 10^{-14}$
reproduction of (Schettino et al., 2015)	$2.0 \cdot 10^{-6}$	$7.7 \cdot 10^{-7}$	$4.5 \cdot 10^{-6}$	$3.8 \cdot 10^{-10}$	$9.1 \cdot 10^{-15}$
results from (Imperi et al., 2018)	$1.1 \cdot 10^{-6}$	$1.0 \cdot 10^{-6}$	$3.3 \cdot 10^{-6}$	$3.2 \cdot 10^{-9}$	$2.9 \cdot 10^{-14}$
reproduction of (Imperi et al., 2018)	$1.1 \cdot 10^{-6}$	$7.5 \cdot 10^{-7}$	$4.8 \cdot 10^{-6}$	$2.5 \cdot 10^{-9}$	$3.4 \cdot 10^{-14}$

Table 3: *Formal uncertainties (1σ) of estimated gravity parameters and solar oblateness when using the method described in section 2, except that only a static $J_{2\odot}$ is included in the virtual reality and the estimation and no other spherical harmonics effects. Simulations are performed for various types of inputs as indicated in the first column.*

	γ	β	η	$J_{2\odot}$	$\frac{G\dot{m}_\odot}{Gm_\odot}$ $[\mathrm{y}^{-1}]$
only using MESSENGER data	$2.3 \cdot 10^{-5}$	$1.9 \cdot 10^{-5}$	$7.2 \cdot 10^{-5}$	$4.8 \cdot 10^{-9}$	$2.9 \cdot 10^{-14}$
only using BepiColombo data	$4.0 \cdot 10^{-6}$	$1.2 \cdot 10^{-6}$	$4.8 \cdot 10^{-6}$	$7.9 \cdot 10^{-10}$	$5.0 \cdot 10^{-15}$
combined data, apriori $\sigma_\gamma = 2.3 \cdot 10^{-5}$	$3.8 \cdot 10^{-6}$	$1.2 \cdot 10^{-6}$	$4.9 \cdot 10^{-6}$	$7.4 \cdot 10^{-10}$	$6.6 \cdot 10^{-16}$
combined data, apriori $\sigma_\gamma = 1.1 \cdot 10^{-6}$	$1.1 \cdot 10^{-6}$	$7.1 \cdot 10^{-7}$	$5.0 \cdot 10^{-6}$	$3.0 \cdot 10^{-10}$	$6.5 \cdot 10^{-16}$

Table 4: *Formal uncertainties (1σ) of estimated gravity parameters and solar oblateness when using the method described in section 2. For the solar spherical harmonics, the time-variable $J_{2\odot}$ is implemented in the virtual reality and the estimation as dictated by the amplitude $A_{J_{2\odot}}$. Simulations are performed for various types of inputs as indicated in the first column.*

	γ	β	η	$J_{2\odot}$	$\frac{G\dot{m}_\odot}{Gm_\odot}$ $[\mathrm{y}^{-1}]$	$A_{J_{2\odot}}$
only using MESSENGER data	$2.3 \cdot 10^{-5}$	$1.9 \cdot 10^{-5}$	$7.2 \cdot 10^{-5}$	$4.8 \cdot 10^{-9}$	$6.0 \cdot 10^{-14}$	$3.1 \cdot 10^{-10}$
only using BepiColombo data	$3.8 \cdot 10^{-6}$	$1.1 \cdot 10^{-6}$	$4.8 \cdot 10^{-6}$	$8.1 \cdot 10^{-10}$	$5.4 \cdot 10^{-15}$	$1.0 \cdot 10^{-10}$
combined data, apriori $\sigma_\gamma = 2.3 \cdot 10^{-5}$	$3.8 \cdot 10^{-6}$	$1.2 \cdot 10^{-6}$	$4.9 \cdot 10^{-6}$	$7.4 \cdot 10^{-10}$	$1.7 \cdot 10^{-15}$	$3.7 \cdot 10^{-11}$
combined data, apriori $\sigma_\gamma = 1.1 \cdot 10^{-6}$	$1.1 \cdot 10^{-6}$	$7.0 \cdot 10^{-7}$	$5.0 \cdot 10^{-6}$	$3.0 \cdot 10^{-10}$	$1.8 \cdot 10^{-15}$	$3.8 \cdot 10^{-11}$

3.3. Perturbations due to $J_{4\odot}$

For $J_{4\odot}$, values in the range from 10^{-9} to 10^{-7} are suggested from heliophysics publications (Rozelot & Damiani, 2011). Even though suggested values for $J_{4\odot}$ can get as high as the values of $J_{2\odot}$, the perturbation is much smaller as it drops off quicker with distance from the Sun (Montenbruck & Gill, 2000). If both zonal coefficients are in the order of magnitude 10^{-7}, the perturbation of $J_{4\odot}$ results in an acceleration acting on Mercury in the order of 10^{-15} m/s^2, whereas $J_{2\odot}$ produces an acceleration in the order of 10^{-12} m/s^2.

Figure 3 has been made to analyse what values of $J_{4\odot}$ produce a detectable change with our observational data. The maximum value of $J_{4\odot}$ suggested in literature is $6.2924 \cdot 10^{-7}$ (Ajabshirizadeh et al., 2008), at which point the change in orbit after 20 years is a few meters, equal to the 1σ noise of MESSENGER observations. The effect that the perturbation produces on the orbit of Mercury is equal to or smaller than noise for realistic values of $J_{4\odot}$. Therefore, it is not possible to distinguish it in the estimation, the effect of the small perturbation can be easily absorbed by the observation noise.

It was attempted to estimate $J_{4\odot}$ when the high estimate of $6.2924 \cdot 10^{-7}$ was implemented. The resulting formal uncertainty on $J_{4\odot}$ came out higher than 100% the value of $J_{4\odot}$, confirming that the perturbation is too small to be constrained with any significant confidence.

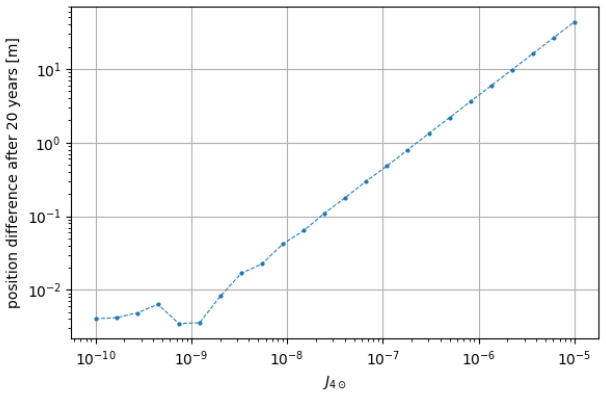

Figure 3: *The difference in final position after 20 years of numerical integration caused by a nonzero value for $J_{4\odot}$. The benchmark orbit used for the comparison is integrated with $J_{4\odot} = 0$.*

3.4. Estimation with a dynamical solar oblateness

Formal uncertainties of the estimated parameters are reported when the periodic component of $J_{2\odot}$ is implemented in our virtual reality. An amplitude $A = 0.563 \cdot 10^{-7}$ was used, a quarter of the value of $J_{2\odot}$ as suggested by (Xu et al., 2017), and it was attempted to estimate $A_{J_{2\odot}}$ alongside the parameters that were estimated in the previous section. The results for the formal uncertainties are reported in table 4.

The resulting formal uncertainty for $A_{J_{2\odot}}$ is $3.7 \cdot 10^{-11}$, 0.017% the value of the zonal coefficient $J_{2\odot}$ itself. The simulation and estimation in this section have been tested for a range of other amplitudes, from $A_{J_{2\odot}} = 0$ to unrealistically high values of $A_{J_{2\odot}} = 1000 \cdot J_{2\odot}$. The resulting true and formal errors are practically identical for any $A_{J_{2\odot}}$, indicating that the ability to constrain the parameter is the same whatever the real value of the periodic component may be. Even if a time-variable component does not exist, the constancy of $J_{2\odot}$ can be constrained to a level of 0.017%.

Compared to the estimation of a static $J_{2\odot}$ in the previous section, the formal uncertainties of the PPN parameters stay unaffected. The time variable gravitational parameter of the Sun $\dot{Gm}_\odot/Gm_\odot$ has a formal error double in value with respect to table 3. The reason is the correlation of 0.92 between the two parameters, indicating that the separate effects are more difficult to distinguish as they have a similar perturbation on the orbit of Mercury. The correlation matrix of the estimated parameters is shown in figure 4.

Figure 4: *Correlation matrix between estimated parameters, when apriori $\sigma_\gamma = 2.3 \cdot 10^{-5}$ and estimating the amplitude.*

3.5. What if $J_{2\odot}$ is periodic, but it is not estimated?

With the suggestion that $J_{2\odot}$ is a dynamic value according to the solar activity cycle, the question can be raised: what happens if a periodic change exists, but it is not estimated? In past experiments it has never been estimated. What are the consequences for the tests of the parameters corresponding to gravitational theory?

Our estimation is executed to test this hypothesis, by setting a dynamic $J_{2\odot}$ in the virtual reality with a mean value $2.25 \cdot 10^7$. The simulation is performed for a range of amplitudes $A_{J_{2\odot}}$ from 0.1% to 100% the value of $J_{2\odot}$. In the estimation algorithm, only a constant value for $J_{2\odot}$ is estimated and a time-variable component is not considered. The resulting true errors of the estimated parameters are plotted against the implemented amplitude in figure 5.

In all of the plots two distinct regions can be identified. At first, for lower values of the amplitude the true error is around the formal error, which is what we would expect of a successful estimation. This indicates that the time-variable perturbation of $J_{2\odot}$ has a negligible effect and no problems will be encountered in the experiment because of it. In the case of only using MESSENGER data this behaviour can be identified in the majority of the plots, because the change in orbit caused by the amplitude is small enough to go undetected when the observation noise is higher.

Secondly, with increasing amplitude the formal errors stay the same while the true errors rise. When using only the BepiColombo or combined data, a clear linear trend in true error can be seen starting from an amplitude of 1% of the value of $J_{2\odot}$. As mentioned in section 2.3.3, high true to formal error ratios are a sign of a bad estimation result, as the true error moves outside the confidence interval indicated by the formal uncertainty.

To give an indication of where formal uncertainties are not reliable any more when using the combined data set (green), we look at the point that the true error is an order of magnitude higher than the formal uncertainty (which means the true estimation error is a value of ten times the formal uncertainty, 10σ). For amplitudes $A_{J_{2\odot}}$ as low as 5% relative to $J_{2\odot}$, the true errors of parameters γ, β are one order of magnitude above the formal uncertainties, and the same holds for the zonal coefficient $J_{2\odot}$ itself. For time-variable gravitational parameter $G\dot{m}_\odot/Gm_\odot$ this point is already reached at 0.2%. It is affected at much lower amplitudes due to the correlation between the parameters (see previous

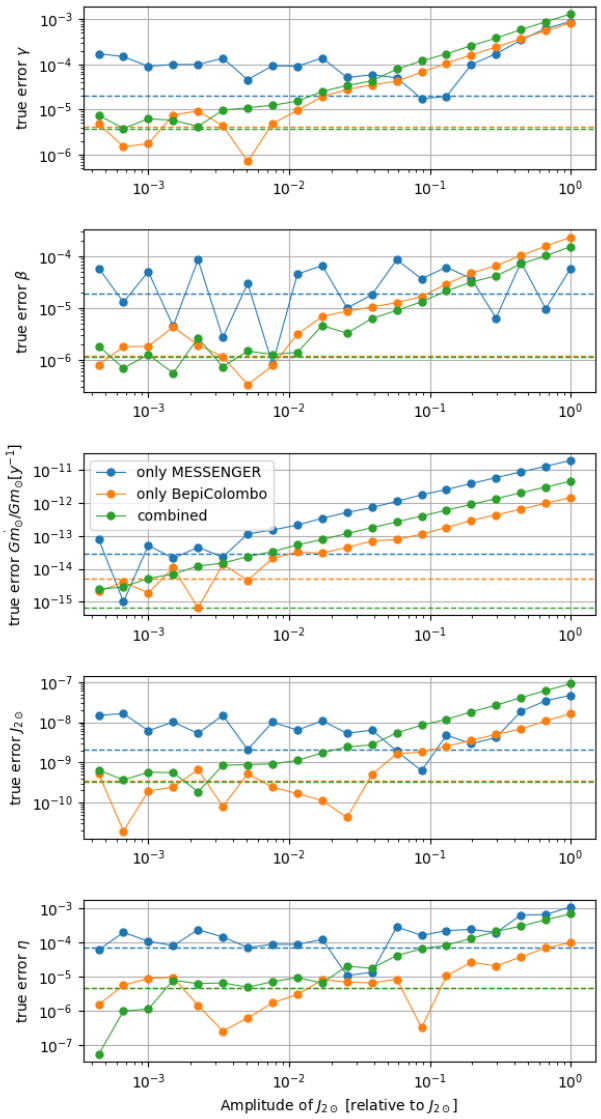

Figure 5: *True estimation errors (absolute values) of parameters when not taking into account a dynamic $J_{2\odot}$, versus the amplitude $A_{J_{2\odot}}$ taken relative to $J_{2\odot}$. The apriori $\sigma_\gamma = 2.3 \cdot 10^{-5}$. The dashed horizontal lines indicate the formal errors, of which the value remains unchanged (up to a relative change of 10^{-5}) independent of amplitude. In all plots except the middle the formal errors of only BepiColombo (orange) and combined data (green) are very similar and therefore the horizontal lines overlap.*

section). Nordtvedt parameter η is the least affected, and the one order of magnitude difference in true and formal errors does not occur until $A_{J_{2\odot}}$ is more than roughly 10% the value of $J_{2\odot}$.

4. Discussion

Before answering the questions about the solar gravity field, the situation without higher-order effects due to the solar shape besides $J_{2\odot}$ was studied. The parameters $\gamma, \beta, \eta, J_{2\odot}, G\dot{m}_\odot/Gm_\odot$, that are conventionally included in similar studies, were estimated using combined data from MESSENGER and BepiColombo. To date, no study has been published that combines the tracking data of both missions in one long-term data set. The first four parameters do however not benefit from this data set compared to only using BepiColombo data. For the time-variable gravitational parameter of the Sun $G\dot{m}_\odot/Gm_\odot$ an improvement of one order of magnitude was found. An improvement in this parameter can be used to test gravitational theories that predict a varying value for the Newtonian constant G such as scalar-tensor theories, and provide more information about the evolution of the universe (Will, 2014; Uzan, 2011).

For realistic values of $J_{4\odot}$ in the range $10^{-9} - 10^{-7}$, changes in the orbit of Mercury are at most a few meters after 20 years. Because MESSENGER tracking data has its noise level in the order of meters, the effect of the zonal effect of degree 4 is not measurable with our data set. It has to be considered too that the uncertainty of other parameters can also easily make up for a change of a few meters, and therefore it is expected that estimating $J_{4\odot}$ with any relevant precision will be hard. It can be concluded that until a mission with similar observational accuracy as BepiColombo reaches Mercury, this effect does not need to be considered.

Next, it is shown that an amplitude $A_{J_{2\odot}}$ of a hypothetical periodic zonal coefficient $J_{2\odot}$ can be estimated with a formal uncertainty of $3.7 \cdot 10^{-11}$, or 0.017% the value of $J_{2\odot}$. The true and formal errors for the amplitude are obtained regardless of the actual value of the amplitude implemented in our virtual reality, meaning that whatever the amplitude is, it can be constrained to this uncertainty. Even if $J_{2\odot}$ is actually constant, its constancy can be constrained to the same uncertainty. The only compromise of estimating the amplitude is that the formal uncertainty of $G\dot{m}_\odot/Gm_\odot$ increases with a factor 2 due to a high correlation between $G\dot{m}_\odot/Gm_\odot$ and $A_{J_{2\odot}}$.

However, the consequences of not including a periodic change of zonal coefficient $J_{2\odot}$ should be seriously considered, as even a small periodic effect can have large consequences in tests of General Relativity. An amplitude of more than a few percent is likely to exist based on publications in heliophysics (Pireaux & Rozelot, 2003; Antia et al., 2007; Rozelot & Damiani, 2011; Xu et al., 2017; Irbah et al., 2019). The results in section 3.5 show that for amplitudes as low as a few percent of $J_{2\odot}$, true errors in the order of 10^{-5} are present in the estimation of PPN parameters γ and β. In past tests of General Relativity using Mercury's perihelion advance, this has not presented a problem, as the formal uncertainties were at best at the same level (e.g. see the results in this work when only using MESSENGER data). However, with the increased accuracy that can be reached with BepiColombo tracking data, the formal uncertainty of PPN parameters γ and β can be brought down by one order of magnitude to the level 10^{-6}. If true errors of order 10^{-5} are caused by not including a periodic $J_{2\odot}$, they can cause problems for the first time when the results come in of the tests using BepiColombo data.

The PPN parameters, which are widely used to test General Relativity, could take on wrong values and be biased towards values that violate General Relativity, while showing a relatively high level of confidence by means of a considerably lower formal uncertainty. The reverse situation could also be imagined: what if the sought-for deviations of General Relativity do exist at the level of accuracy that BepiColombo can measure, but the PPN parameters are biased towards General Relativity due to the periodic change in the solar shape? In any case, the scientific community studying gravitational physics would be put on the wrong path.

It is therefore strongly advised to estimate a periodic change of the solar oblateness in experiments of gravitational physics. Even if the periodic change is too low and negligible, constraining it would confirm that there is no risk of getting biased results for experiments of General Relativity. In addition, constraining the value for parameter $J_{2\odot}$ and a possible variation along the solar cycle is of importance to research in heliophysics. Much is unknown about the interior and dynamics of the Sun, and getting stringent bounds on the oblateness will help confirm or reject models for the structure of the Sun.

5. Conclusion

The aim of this study is to investigate different configurations of the solar spherical harmonics gravity field that are suggested in the field of heliophysics, and attempt to determine whether or not it is possible to confirm or deny their existence with tracking data from MESSENGER and BepiColombo missions to Mercury. In addition, it is investigated what the consequence is of ignoring this effect.

To achieve this goal, a numerical simulation of Mercury's trajectory and the spacecraft tracking was set up as well as a parameter estimation algorithm. In spite of simplifications that had to be done because of limited resources, validation showed that our setup is of comparable quality to other publications on the subject (Genova et al., 2018; Schettino et al., 2015; Imperi et al., 2018).

Combining the data set of MESSENGER and BepiColombo results in a factor 2 decrease of the formal uncertainty of a time-variable gravitational parameter of the Sun. Because the resulting formal uncertainties for the other parameters are unchanged, it can be concluded that it is worthwhile to include the MESSENGER data set in relativity experiments based on BepiColombo data.

The effect of a zonal coefficient $J_{4\odot}$ is lower than the noise level of the tracking data, and therefore higher order zonal effects of the Sun can be safely ignored in experiments of gravitational physics with BepiColombo data.

A periodic change in the zonal coefficient $J_{2\odot}$ based on the solar magnetic activity cycle does however have significant effects on the orbit of Mercury, to the point that it can influence results of gravitational experiments done with BepiColombo data. It is urged to estimate the periodic change in the coefficient $J_{2\odot}$ in such experiments, as suggested values for a periodic change from heliophysics can have a significant effect on the estimation of relativity parameters. This could lead to a false confirmation or rejection of the perihelion advance effect as predicted by General Relativity.

References

Ajabshirizadeh, A., et al. (2008). Contribution of the Solar Magnetic Field on Gravitational Moments. *Scientia Iranica*, *15*(1).

Alessi, E., et al. (2012). Desaturation manoeuvres and precise orbit determinationfor the BepiColombo mission. *Monthly Notices of the Royal Astronomical Society*, *423*(3), 2270-2278.

Antia, H. M., et al. (2007). Temporal Variations in the Sun's Rotational Kinetic Energy. *Astronomy & Astrophysics*, *477*(2).

Armstrong, J., & Kuhn, J. R. (1999). Interpreting the Solar Limb Shape Distortions. *The Astrophysical Journal*, *525*, 533-538.

Ashby, N., et al. (2007). Future gravitational physics tests from ranging to the BepiColombo Mercury planetary orbiter. *Physical Review D*, *75*(2).

Bertotti, B., et al. (2003). A test of general relativity using radio links with the Cassini spacecraft. *Nature*, *425*, 374-376.

Cappuccio, P., et al. (2020). Report on first inflight data of bepicolombo's mercury orbiter radio-science experiment. *IEEE Transactions on Aerospace and Electronic Systems*, 1-1.

Cicalo, S., et al. (2016). The BepiColombo MORE gravimetry and rotation experimentswith theORBIT14 software. *Monthly Notices of the Royal Astronomical Society*, *457*(2).

Damiani, C., et al. (2011). A brief history of the solar oblateness. A review. *Journal of Atmospheric and Solar-Terrestrial Physics*, *73*, 241-250.

Dekking, F., et al. (2005). *A Modern Introduction to Probability and Statistics*. Springer.

Dirkx, D., et al. (2019). Propagation and estimation of the dynamical behaviour of gravitationally interacting rigid bodies. *Astrophysics and Space Science*, *364*(37).

Einstein, A. (1916). Die Grundlage der allgemeinen Relativitätstheorie. *Annalen der Physik*, *354*(7), 769-822.

Fienga, A., et al. (2009). INPOP08, a 4-D planetary ephemeris: from asteroid and time-scale computations to ESA Mars Express and Venus Express contributions. *Astronomy and Astrophysics*, *507*(3), 1675-1686.

Fienga, A., et al. (2011). The INPOP10a planetary ephemeris and its applications in fundamental physics. *Celestial Mechanics and Dynamical Astronomy*, *111*, 363-385.

Fienga, A., et al. (2015). Numerical estimation of the sensitivity of INPOPplanetary ephemerides to general relativity parameters. *Celestial Mechanics and Dynamical Astronomy*, *123*, 325-349.

Fienga, A., et al. (2019). *INPOP19a Planetary Ephemerides scientific notes* (Tech. Rep.). Institute for Celestial Mechanics and Computation of Ephemerides.

Fivian, M. D., et al. (2008). Solar Shape Measurements from RHESSI: A Large Excess Oblateness. *Science*, *322*, 560-562.

Folkner, W. M., et al. (2014). *The Planetary and Lunar Ephemerides DE430 and DE431* (Tech. Rep.). Jet Propulsion Laboratory. (IPN Progress Report 42-196)

Genova, A., et al. (2008). Mercury radio science experiment of the mission bepicolombo. *Memoire della Società Astronomica Italiana*, *75*, 282-286.

Genova, A., et al. (2018). Solar system expansion and strong equivalence principle as seen by the NASA MESSENGER mission. *Nature communications*, *9*(289).

Godier, S., & Rozelot, J. P. (1999). Relationships between the quadrupole moment and the internal layers of the Sun. In *Magnetic fields and solar processes* (Vol. 9, p. 111-115).

Iess, L., & Boscagli, G. (2001). Advanced radio science instrumentation for the mission BepiColombo to Mercury. *Planetary and Space Science*, *49*(14-15), 1597-1608.

Iess, L., et al. (2009). MORE: An advanced tracking experiment for the exploration of Mercury with the mission BepiColombo. *Acta Astronautica*, *65*(5-6), 666-675.

Imperi, L., & Iess, L. (2017). The determination of the post-Newtonian parameter γ during the cruise phase of BepiColombo. *Classical and Quantum Gravity*, *34*(7).

Imperi, L., Iess, L., & Mariani, M. J. (2018). Analysis of the geodesy and relativity experiments of BepiColombo. *Icarus*, *301*, 9-25.

Iorio, L. (2014). Constraining the preferred-frame α_1, α_2 parameters from solar system planetary precessions. *International Journal of Modern Physics D*, *23*(1).

Irbah, A., et al. (2019). Variations of Solar Oblateness with the 22yr Magnetic Cycle Explain Apparently Inconsistent Measurements. *The Astrophysical Journal LEtters*, *875*(2).

Kopeikin, S. M., et al. (2011). *Relativistic Celestial Mechanics of the Solar System*. Wiley VCH.

Kuhn, J. R., et al. (2012). The Precise Solar Shape and Its Variability. *Science*, *337*(6102), 1638-1640.

Le Verrier, U. J. (1859). Theorie du mouvement de mercure. *Annales de l'Observatoire imperial de Paris*, *5*.

Mattingly, D. (2005). Modern tests of lorentz invariance. *Living Reviews in Relativity*, *8*(5).

Mazarico, E., et al. (2014). The gravity field, orientation, and ephemeris of Mercury from MESSENGER observations after three years in orbit. *Journal of Geophysical Research: Planets*, *119*(12).

Mecheri, R., et al. (2009). New values of gravitational moments J2 and J4 deduced from helioseismology. *Solar Physics*, *222*(2).

Meftah, M., et al. (2016). On HMI solar oblateness during solar cycle 24 and impact of the space environment on results. *Advances in Space Research*, *58*(7), 1425-1440.

Milani, A., et al. (2002). Testing general relativity with the BepiColombo radio science experiment. *Physical Review D*, *66*(8).

Montenbruck, O., & Gill, E. (2000). *Satellite Orbits - Models, Methods and Applications*. Springer. (Corrected 3rd printing 2005)

NOAA Space Weather Prediction Center. (2020, september). Solar Cycle Progression. Retrieved from `https://www.swpc.noaa.gov/products/solar-cycle-progression`

Park, R. S., et al. (2017). Precession of Mercury's Perihelion from Ranging to the MESSENGER Spacecraft. *The Astronomical Journal*, *153*(3).

Petit, G., & Luzum, B. (2010). *IERS Conventions*. Frankfurt am Main: Verlag des Bundesamts für Kartographie und Geodäsie. (IERS Technical Note 36 Chapter 10)

Pijpers, F. P. (1998). Helioseismic determination of the solar gravitational quadruple moment. *Monthly Notices of the Royal Astronomical Society*, *297*, L76-L80.

Pireaux, S., & Rozelot, J.-P. (2003). Solar quadruple moment and purely relativistic gravitation contributions to Mercury's perihelion advance. *Astrophysics and Space Science*, *284*(4), 1159-1194.

Pitjeva, E. V. (2005). Relativistic Effects and Solar Oblateness from Radar Observations of Planets and Spacecraft. *Astronomy Letters*, *31*(5), 340-349.

Pitjeva, E. V., & Pavlov, D. (2017). *EPM2017 and EPM2017H* (Tech. Rep.). Institute of Applied Astronomy, Russion Academy of Sciences. (`http://iaaras.ru/en/dept/ephemeris/epm/2017/`)

Pitjeva, E. V., & Pitjev, N. P. (2013). Relativistic effects and dark matter in the solar system from observations of planets and spacecrafts. *Monthly Notices of the Royal Astronomical Society*, *432*(4), 3431-3437.

Pitjeva, E. V., & Pitjev, N. P. (2014). Development of planetary ephemerides EPM and their applications. *Celestial Mechanics and Dynamical Astronomy*, *119*(3-4).

Roxburgh, I. W. (2001). Gravitational multipole moments of the Sun determined from helioseismic estimates of the internal structure and rotation. *Astronomy & Astrophysics*, *377*, 668-690.

Rozelot, J.-P., & Damiani, C. (2011). History of solar oblateness measurements and interpretation. *The European Physical Journal H*, *36*(3), 407-436.

Rozelot, J.-P., et al. (2009). Probing the solar surface: the oblateness and astrophysical consequences. *The Astrophysical Journal*, *703*, 1791-1796.

Schettino, G., et al. (2015). The relativity experiment of MORE: Global full-cycle simulation and results. In *2015 IEEE Metrology for Aerospace (MetroAeroSpace)* (p. 141-145).

Shao, L., et al. (2013). A new limit on local Lorentz invariance violation of gravity from solitary pulsars. *Classical and Quantum Gravity*, *30*(16).

Shao, L., & Wex, N. (2012). New tests of local Lorentz invariance of gravity with small-eccentricity binary pulsars. *Classical and Quantum Gravity*, *29*(21).

Shapiro, I. I. (1999). A century of relativity. *Reviews of Modern Physics*, *71*(2).

SILSO World Data Center. (2020, september). The International Sunspot Number. *International Sunspot Number Monthly Bulletin and online catalogue*. Retrieved from `http://www.sidc.be/silso/`

Uzan, J.-P. (2011). Varying constants, gravitation and cosmology. *Living Reviews in Relativity*, *14*(2).

Verma, A. K., et al. (2014). Use of messenger radioscience data to improve planetary ephemeris and to test general relativity. *Astronomy & Astrophysics*, *561*(A115).

Viswanathan, V., et al. (2018). The new lunar ephemeris INPOP17a and its application to fundamental physics. *Monthly Notices of the Royal Astronomical Society*, *476*(2), 1877-1888.

Will, C. M. (1981). *Theory and Experiment in Gravitational Physics*. Cambridge University Press.

Will, C. M. (2014). The Confrontation between General Relativity and Experiment. *Living Reviews in Relativity*, *17*(4).

Will, C. M., & Nordtvedt, K. (1972). Conservation Laws and Preferred Frames in Relativistic Gravity. I. Preferred-Frame Theories and an Extended PPN Formalism. *The Astrophysical Journal*, *177*, 757-774.

Williams, J. G., et al. (2012). Lunar laser ranging tests of the equivalence principle. *Classical and Quantum Gravity*, *29*(18).

Xu, Y., et al. (2017). Perihelion precession caused by solar oblateness variation in equatorial and ecliptic coordinate systems. *Monthly Notices of the Royal Astronomical Society*, *472*(3), 2686-2693.

Table 5: *Selected attempts to determine $J_{2\odot}$ over the last 25 years, as shown graphically in figure 1. "H" and "P" are labels to indicate whether a value was found in the field of heliophysics (H) or by using observations of planetary orbits (P). For comprehensive lists of attempts, see (Pireaux & Rozelot, 2003) and (Rozelot & Damiani, 2011).*

Publication		$\mathbf{J_{2\odot}}$	$\mathbf{1\sigma}$
Fienga et al., 2019	P	$2.01 \cdot 10^{-7}$	$1 \cdot 10^{-9}$
Genova et al., 2018	P	$2.25 \cdot 10^{-7}$	$2 \cdot 10^{-9}$
Park et al., 2017	P	$2.25 \cdot 10^{-7}$	$9 \cdot 10^{-9}$
Pitjeva & Pavlov, 2017	P	$2.37 \cdot 10^{-7}$	-
Verma et al., 2014	P	$2.4 \cdot 10^{-7}$	$2 \cdot 10^{-8}$
Fienga et al., 2015	P	$2.3 \cdot 10^{-7}$	$2.5 \cdot 10^{-8}$
Folkner et al., 2014	P	$2.11 \cdot 10^{-7}$	-
Pitjeva & Pitjev, 2014	P	$2.22 \cdot 10^{-7}$	$2.3 \cdot 10^{-8}$
Fienga et al., 2011	P	$2.4 \cdot 10^{-7}$	$2.5 \cdot 10^{-8}$
Fienga et al., 2009	P	$1.82 \cdot 10^{-7}$	$4.9 \cdot 10^{-8}$
Mecheri et al., 2009	H	$2.21 \cdot 10^{-7}$	-
Fivian et al., 2008	H	$1.65 \cdot 10^{-7}$	$9.73 \cdot 10^{-8}$
Antia et al., 2007	H	$2.22 \cdot 10^{-7}$	$9 \cdot 10^{-10}$
Pitjeva, 2005	P	$1.9 \cdot 10^{-7}$	$3 \cdot 10^{-5}$
Roxburgh, 2001	H	$2.21 \cdot 10^{-7}$	-
Godier & Rozelot, 1999	H	$1.6 \cdot 10^{-7}$	$4 \cdot 10^{-9}$
Armstrong & Kuhn, 1999	H	$2.22 \cdot 10^{-7}$	-
Pijpers, 1998	H	$2.18 \cdot 10^{-7}$	$6 \cdot 10^{-9}$

3

Conclusions and Recommendations

3.1. Conclusions

In the discussion of the journal article, the answers to the four research questions are given. In this conclusion of the thesis work, the answers will be quickly repeated and afterwards, conclusions will be given in the greater context of the introduction given in chapter 1. The research questions were: **Using combined tracking data of the MESSENGER and BepiColombo missions in a parameter estimation algorithm,**

1. **to what accuracy can parameters of General Relativity and the solar quadruple moment $J_{2\odot}$ be determined?**
   Using the combined data set does not have any advantage for the estimation of the parameters, compared to only using BepiColombo data. The only exception is the time variable gravitational parameter $Gm_{\odot}$, of which the formal uncertainty is two orders of magnitude lower.

2. **what dynamic values for $J_{2\odot}$ can be detected?**
   The estimation of the amplitude has a true error of $4 \cdot 10^{-11}$, or about 0.017% the value of $J_{2\odot}$ itself, regardless of the value of the amplitude.

3. **can higher order effects due to other zonal coefficients $J_{n\odot}$ be detected?**
   The next zonal effect, $J_{4\odot}$, causes a difference in the orbit of Mercury between the two missions that is too small to be detected using the observations of the missions.

4. **if higher order effects do exist but are not considered in gravitational experiments, what will be the impact in the estimation of relativistic parameters?**
   If the amplitude is higher than 1% of the value of $J_{2\odot}$ and it is not considered in an estimation, it will lead to true errors for parameters of gravitational theory that are higher than twice the formal errors, meaning that the actual value of the parameter lies outside of a 95% confidence interval.

To conclude, the hypothesis from the introduction has a positive result in the case of the time variable gravitational oblateness of the Sun: it can have a relevant effect on the tests of General Relativity that will be done using BepiColombo data, and it should be taken into account in experiments that use BepiColombo data. If not modelled correctly, it is possible that the experiments to prove General Relativity can have a result that is a false negative. The consequences of such results could be comparable to the controversy around General Relativity that was present in the 1960's, where whole other theories of gravity were developed to do so. In order to prevent this, and in the interest of testing gravity as accurately as possible, the solar shape should be further studied and included in such experiments.

Only if the time-variable component is smaller than approximately 1% the value of $J_{2\odot}$, the general hypothesis is false: the variability does not matter and it can be safely ignored. However, because a decent estimate for an upper limit of the variability of the oblateness is not known at this time, it should always be considered in future experiments, at the very least to obtain such an upper limit and the effect can be ruled out.

Of course, the assumption of General Relativity being right is implied in this work, as it often is done in such publications until proven wrong. The conclusions however work in any way in this paper, if the

parameters are not the values predicted by General Relativity, a high true error could coincidentally lead us to believe that they are. Correct modelling and measuring eventually will bring out the truth.

3.2. Recommendations

Based on the results and conclusions presented in this work a few recommendations can be made:

- First and foremost, as is clear from the conclusion, it is urged to colleagues in this field of research, as well as developers of ephemerides, to take note of the possibility of a time-variable solar oblateness. At this point the possibility of this effect cannot be ruled out, and finding constraints of it based on observational data would be very valuable to rule out the possibility of false results of experiments.

- Concerning the zonal effects of degree four or higher, there is currently less reason for concern, although it is recommended to keep an eye on any developments from the field of heliophysics. In the future, if tracking data becomes available of the accuracy of BepiColombo or better, it should be reanalysed whether the $J_{4\odot}$ effect could play a role. Figure 3 of the journal article indicates what accuracy is needed to constrain the effects of certain $J_{4\odot}$ values. This figure indicates the change in 20 years, however it can be interpolated or extrapolated as the position change scales linearly with time.

- In general, a recommendation can be made to those who design experiments to test gravitational theory in the solar system, to work more closely together with the field of heliophysics. In this way, true understanding of the problem of the solar shape can be created. In that case it will hopefully not be written off just a nuisance for which an assumption has to be made, but proper attention will be devoted to it in experiments of gravity. Good modelling of the problem and good experiments to measure the phenomena will ultimately benefit both fields in their individual research.

- In this work uncertainties in certain parameters were studied could affect the experiments of gravity. When studying the effects during this work it was found that two in particular can have a significant effect on the results:

  - The first is the angular momentum of the Sun, for which in most experiments a constant value is used from one reference [45], but not much research is published on the solar anular momentum. The uncertainty from [45] is only 1%, but it is a dominant factor in the Lense-Thirring effect, which is known to correlate with PPN parameter β.
  - The uncertainties of the masses of the asteroids have very high values relative to the masses themselves, due to which the magnitude point mass accelerations of the asteroids have a very high uncertainty. Like many effects the asteroids also cause an advance in the perihelion of Mercury, and formal errors of all parameters are affected by it.

  Improving the apriori uncertainty on these two types of parameters can improve the results of gravitational tests by a significant amount, and therefore dedicated research to further measure them can be of great value. This would perhaps be one of the only ways to obtain smaller bounds for various gravity parameters in the future without sending new space missions to Mercury or other planets.

- The periodic part of the solar gravitational oblateness is currently modelled as a simple sine. It should be emphasised that this is a simplification of the real problem, which is that the magnetic solar activity of the Sun drives the periodic part of the oblateness. Magnetic solar activity generally follows a cycle of 11 years, but individual cycles can be shorter or longer and the magnetic activity can be higher or lower compared to others [22]. To properly model the activity cycle, the underlying parameter should not be time but a measure of solar activity, for which often the sunspot number is used which is depicted in figure 2 of the journal article. How this measure of solar activity relates to an increase in oblateness is a challenge to tackle, but the relation between the two is being investigated [28]. The sinusoidal variation was mainly used in this work as a means to show what the impact of a variable oblateness could be, but its value at any specific points may certainly be off.

- This work has been done with Mercury as the only test body. Additional test bodies (planets or spacecraft in heliocentric orbit) can be added to extend the experiment. The advantage is that the relativistic effects and perturbations due to the solar shape can be decorrelated, as they scale differently based on semi-major axis and eccentricity of the planets' orbit. The disadvantage is that both effects are weaker

on test bodies because they scale inversely with distance from the Sun and therefore harder to pick up. In addition, the state of more planets have to be estimated and if the observations of other planets are not as accurate, this will harm the accurate estimation of Mercury's state. Probably very large data sets are needed to surpass the tests done only with Mercury. For certain, the developers of ephemerides are eagerly waiting to add the BepiColombo data to improve their huge data sets, which can be used for tests of gravity.

3.3. Testing General Relativity in the Solar System: a short outlook

The potential of the data brought by the BepiColombo mission has been elaborated to great detail in this work. On the horizon that we can see currently, there are no missions planned dedicated to testing gravity in the Solar System, and there seems to be no space mission planned of which the data is good enough to produce a test of General Relativity that can surpass BepiColombo. However, tracking capabilities of interplanetary missions in general are improving in quality. This will produce a larger base of observations of the whole Solar System which can work in synergy with the Mercury data. In addition, some upcoming opportunities can be identified specifically that could work very well in combination with the observations of Mercury to produce even better estimates of PPN parameters or the solar oblateness, and as a very broad recommendation they are shortly named in this section.

There is one other ESA mission currently returning data that promises to be very useful: GAIA. While the GAIA mission is mainly focused on observing stars in our galaxy, tens of thousands asteroids are picked up in the spacecraft observations as well, resulting in millions of observations. The variety of asteroid orbits is much higher than the planets, for example the eccentricity or inclination of the orbits, which will help decorrelate the effects due to the relativistic perturbation and the solar oblateness. The use of the GAIA data has been explored already by [24], which shows that some exotic effects of gravitational theories can also be detected using the variety of asteroid orbits, which the planets are less suitable for. Also, the first data of GAIA is being included in the new version of the INPOP ephemeris [17]. At a first glance, it seems that there is a lot more potential in the data, especially when the final data is released (currently planned in 2022[1]). The challenge is finding a way to include all the asteroids and their observations in an estimation. Numerically integrating orbits of tens of thousands of asteroids and then performing the matrix operations for millions of observations requires a huge amount of computational power, and perhaps new and innovative methods are required to tackle this problem instead of the traditional way of parameter estimation that is already done for decades.

Similarly, it can be expected that an increasing amount of test bodies in the Solar System can be added to gravity experiments, because there seems to be a large focus in the future on space missions that visit small bodies such as dwarf planets, comets and asteroids. While the GAIA observations are sparse, orbiters of small bodies could provide large data sets of certain bodies to implement in gravity experiments. An advantage of studying small bodies in general is that the uncertainty of the orbits and masses will decrease over time, which will lead to an improvement in ephemerides of the planets as well.

[1] https://www.cosmos.esa.int/web/gaia/release

A

Acceleration Models

As described in section 2.1 of the journal article, the numerical integration of Mercury is done with a variety of acceleration terms. In TUDAT, basic acceleration models were already present that are applicable in many situations. However, some acceleration models had to be added to TUDAT for this project in particular. This appendix aims to describe acceleration models that were added to TUDAT for this project. In particular, partial derivatives of the acceleration terms are needed with respect to parameters that are to be estimated. These partials have been analytically derived and will be described.

A.1. Lense-Thirring acceleration correction

The Lense-Thirring effect (also called frame-dragging or gravitomagnetic effect) is the effect that a spinning body can warp spacetime around it and therefore influence test bodies in its vicinity. The Lense-Thirring acceleration correction was already implemented in TUDAT, according to the following relation [44, eq. 10.12]:

$$\mathbf{a}_{\text{LT}} = (1+\gamma)\frac{GM}{c^2 r^3}\left[\frac{3}{r^2}(\mathbf{r}\times\mathbf{v})(\mathbf{r}\cdot\mathbf{S}_\odot) + (\mathbf{v}\times\mathbf{S}_\odot)\right] \tag{A.1}$$

where gravitational parameter GM and mass-normalized angular momentum vector $\mathbf{S}_\odot$ belong to the central body, and the correction is calculated for the accelerated body. $\mathbf{a}, \mathbf{v}$ and $\mathbf{r}$ stand for acceleration, velocity and position respectively.

Partial derivatives were not yet implemented into TUDAT for this acceleration term. For the derivatives of the cross products, use is made of the matrix notation of a vector such that the cross product can be written as a dot product:

$$\mathbf{r}\times\mathbf{v} = \begin{bmatrix} 0 & v_z & -v_y \\ -v_z & 0 & v_x \\ v_y & -v_x & 0 \end{bmatrix}\mathbf{r} = \left[\mathbf{v}^\times\right]^T\mathbf{r} \qquad \frac{\partial}{\partial\mathbf{r}}(\mathbf{r}\times\mathbf{v}) = \left[\mathbf{v}^\times\right]^T \tag{A.2}$$

$$\mathbf{r}\times\mathbf{v} = \begin{bmatrix} 0 & -z & y \\ z & 0 & -x \\ -y & x & 0 \end{bmatrix}\mathbf{v} = \left[\mathbf{r}^\times\right]\mathbf{v} \qquad \frac{\partial}{\partial\mathbf{v}}(\mathbf{r}\times\mathbf{v}) = \left[\mathbf{r}^\times\right] \tag{A.3}$$

Using this result, the partial derivatives can be derived with respect to position, velocity, gravitational parameter and PPN parameter γ respectively:

$$\begin{aligned}\frac{\partial\mathbf{a}_{\text{LT}}}{\partial\mathbf{r}} =& 3\left(1+\gamma\right)\frac{GM}{c^2 r^5}\left[\frac{-2}{r^2}(\mathbf{r}\times\mathbf{v})(\mathbf{r}\cdot\mathbf{S}_\odot)\mathbf{r}^T + (\mathbf{r}\cdot\mathbf{S}_\odot)\left[\mathbf{v}^\times\right]^T + (\mathbf{r}\times\mathbf{v})\mathbf{S}_\odot^T\right] \\ & - 3(1+\gamma)\frac{GM}{c^2 r^3}\left[\frac{3}{r^2}(\mathbf{r}\times\mathbf{v})(\mathbf{r}\cdot\mathbf{S}_\odot) + (\mathbf{v}\times\mathbf{S}_\odot)\right]\frac{\mathbf{r}^T}{r^2}\end{aligned} \tag{A.4}$$

$$\frac{\partial\mathbf{a}_{\text{LT}}}{\partial\mathbf{v}} = (1+\gamma)\frac{GM}{c^2 r^3}\left[\frac{3}{r^2}(\mathbf{r}\cdot\mathbf{S}_\odot)\left[\mathbf{r}^\times\right] + \left[\mathbf{S}_\odot^\times\right]^T\right] \tag{A.5}$$

$$\frac{\partial\mathbf{a}_{\text{LT}}}{\partial GM} = (1+\gamma)\frac{1}{c^2 r^3}\left[\frac{3}{r^2}(\mathbf{r}\times\mathbf{v})(\mathbf{r}\cdot\mathbf{S}_\odot) + (\mathbf{v}\times\mathbf{S}_\odot)\right] \tag{A.6}$$

$$\frac{\partial \mathbf{a}_{\text{LT}}}{\partial \gamma} = \frac{GM}{c^2 r^3}\left[\frac{3}{r^2}(\mathbf{r}\times\mathbf{v})(\mathbf{r}\cdot\mathbf{S}_\odot) + (\mathbf{v}\times\mathbf{S}_\odot)\right] \tag{A.7}$$

In addition, the magnitude of the solar angular momentum $S_\odot$ is implemented as a consider parameter, for which also partial derivatives are required. It shows up through $\mathbf{S}_\odot$, the mass-normalised angular momentum vector, which is calculated as follows:

$$\mathbf{S}_\odot = \frac{S_\odot}{M_\odot}\cdot\mathbf{n}_S \tag{A.8}$$

where $\mathbf{n}_S$ is the unit vector of the angular momentum vector of the Sun. The partial derivative with respect to the angular momentum magnitude becomes:

$$\frac{\partial \mathbf{a}_{\text{LT}}}{\partial S_\odot} = (1+\gamma)\frac{GM}{c^2 r^3}\left[\frac{3}{r^2}(\mathbf{r}\times\mathbf{v})\left(\mathbf{r}\cdot\frac{\mathbf{n}_S}{M_\odot}\right) + \left(\mathbf{v}\times\frac{\mathbf{n}_S}{M_\odot}\right)\right] \tag{A.9}$$

A.2. Time-variable gravitational parameter

The acceleration due to the changing gravitational parameter of the Sun is given by the following equation [21, eq. 11]:

$$\mathbf{a}^{G\dot{M}}_{\text{M}\odot} \cong -GM_\odot\left(\frac{G\dot{M}_\odot}{GM_\odot}\Delta t\right)\frac{\mathbf{r}_{\text{M}\odot}}{r^3_{\text{M}\odot}} \tag{A.10}$$

where $\frac{G\dot{M}_\odot}{GM_\odot}$ is the term that is meant with the definition *time-variable gravitational parameter* and Δt is the time since reference epoch J2000. A minus-sign is added with respect to the equation given in [21], as in the TUDAT definition of the relative position vector $\mathbf{r}_{\text{M}\odot}$ acceleration due to central gravity should be negative for a positive position input. With this changed sign, a decreasing gravitational parameter (negative $\frac{G\dot{M}_\odot}{GM_\odot}$) causes a positive acceleration, i.e. causes the accelerated body to move away from the Sun.

This expression only provides an approximation of what effects a time-variable gravitational parameter would cause. More specifically, this expression corrects the central gravity acceleration of the Sun on Mercury due to a change in gravitational parameter. Other changes caused by this effect are neglected, as the Solar central gravity term is the most dominant acceleration term, and the next acceleration term due to the Sun (Schwarzschild correction) is smaller by a factor of approximately 10^{-7}. A correction on this term would not have significant influence compared to the central gravity term.

The partial derivatives with respect to position, gravitational parameter, and time-variable gravitational parameter are respectively:

$$\frac{\partial \mathbf{a}^{G\dot{M}}_{\text{M}}}{\partial \mathbf{r}_{\text{M}\odot}} \cong -GM_\odot\left(\frac{G\dot{M}_\odot}{GM_\odot}\Delta t\right)\left(\frac{1}{r^3_{\text{M}\odot}}\mathbf{I} - 3\mathbf{r}_{\text{M}\odot}\frac{\mathbf{r}^T_{\text{M}\odot}}{r^5_{\text{M}\odot}}\right) \tag{A.11}$$

$$\frac{\partial \mathbf{a}^{G\dot{M}}_{\text{M}}}{\partial GM_\odot} \cong \left(\frac{G\dot{M}_\odot}{GM_\odot}\Delta t\right)\frac{\mathbf{r}_{\text{M}\odot}}{r^3_{\text{M}\odot}} \tag{A.12}$$

$$\frac{\partial \mathbf{a}^{G\dot{M}}_{\text{M}}}{\partial\left(\frac{G\dot{M}_\odot}{GM_\odot}\right)} \cong GM_\odot\Delta t\frac{\mathbf{r}_{\text{M}\odot}}{r^3_{\text{M}\odot}} \tag{A.13}$$

where $\mathbf{I}$ is the identity matrix of size 3×3.

A.3. Strong Equivalence Principle Violation

In conventional ephemeris models it is assumed that inertial and gravitational masses of bodies are equal, an assumption that is only valid when the Strong Equivalence Principle (SEP) is correct. Violations of the SEP are usually expressed using the Nordtvedt parameter η. The parameter can be expressed as a linear combination of PPN parameters through the Nordtvedt equation [56, eq. 68]:

$$\eta = 4(\beta-1) - (\gamma-1) - \alpha_1 - \frac{2}{3}\alpha_2 \tag{A.14}$$

where it is assumed that total momentum is conserved, i.e. PPN parameters $\alpha_3, \zeta_1, \zeta_2, \xi = 0$. The largest perturbation caused by a SEP violation is that SSB has to be redefined (see [21, 39]), which influences the position of the Sun according to the following expression [21, eq. 9]:

$$\mathbf{r}_{\odot}^{SEP} = -\frac{1}{\mu_{\odot}\left(1-\eta\frac{\Omega_{\odot}}{M_{\odot}c^2}\right)}\sum_{j\neq\odot}\left(1-\eta\frac{\Omega_j}{M_j c^2}\right)\mu_j\mathbf{r}_j \tag{A.15}$$

where the gravitational self-energies Ω_i of the bodies are taken as described in [21].

Recalculating the SSB is not an option in our simulation, as the SSB and body positions are not calculated but obtained from ephemeris DE430 [18]. Therefore, the approach is to get a *correction* on the position of the Sun $\mathbf{r}_{\odot}$, which can be derived by comparing with the situation $\eta = 0$:

$$\begin{aligned}\Delta\mathbf{r}_{\odot}^{SEP} &= (\mathbf{r}_{\odot})_{\eta\neq 0} - (\mathbf{r}_{\odot})_{\eta=0} \\ &= \left[-\frac{1}{\mu_{\odot}\left(1-\eta\frac{\Omega_{\odot}}{M_{\odot}c^2}\right)}\sum_{j\neq\odot}\left(1-\eta\frac{\Omega_j}{M_j c^2}\right)\mu_j\mathbf{r}_j\right] - \left[-\frac{1}{\mu_{\odot}}\sum_{j\neq\odot}\mu_j\mathbf{r}_j\right]\end{aligned} \tag{A.16}$$

The term containing η and properties of the Sun is usually very small. A Taylor series expansion around zero can be used to simplify the equation and combine the terms:

$$\frac{1}{\left(1-\eta\frac{\Omega_{\odot}}{M_{\odot}c^2}\right)} = 1+\eta\frac{\Omega_{\odot}}{M_{\odot}c^2} + O\left(\left(\eta\frac{\Omega_{\odot}}{M_{\odot}c^2}\right)^2\right) \tag{A.17}$$

where it is assumed that $O\left(\left(\eta\frac{\Omega_{\odot}}{M_{\odot}c^2}\right)^2\right)$ and higher order terms can be neglected. From substitution follows:

$$\begin{aligned}\Delta\mathbf{r}_{\odot}^{SEP} &= \left[-\frac{\left(1+\eta\frac{\Omega_{\odot}}{M_{\odot}c^2}\right)}{\mu_{\odot}}\sum_{j\neq\odot}\left(1-\eta\frac{\Omega_j}{M_j c^2}\right)\mu_j\mathbf{r}_j\right] - \left[-\frac{1}{\mu_{\odot}}\sum_{j\neq\odot}\mu_j\mathbf{r}_j\right] \\ &= -\frac{1}{\mu_{\odot}}\sum_{j\neq\odot}\left[\left(1+\eta\frac{\Omega_{\odot}}{M_{\odot}c^2}\right)\left(1-\eta\frac{\Omega_j}{M_j c^2}\right)\mu_j\mathbf{r}_j - \mu_j\mathbf{r}_j\right] \\ &= -\frac{\eta}{\mu_{\odot}c^2}\sum_{j\neq\odot}\left(\frac{\Omega_{\odot}}{M_{\odot}} - \frac{\Omega_j}{M_j}\right)\mu_j\mathbf{r}_j\end{aligned} \tag{A.18}$$

In the last step, the bracket multiplication result of the two terms containing η is neglected as it leads to an insignificantly low value of $O\left(\eta^2 c^{-4}\right)$. The results of equations A.16 and A.18 are compared in a simulation with $\eta = -7\cdot 10^{-5}$ and the simplification leads to an error that is at maximum 0.01% of $\Delta\mathbf{r}_{\odot}^{SEP}$, which verifies that the simplification will not lead to significant errors in the simulation.

Because of the correction on the position of the Sun, the relative position vector of Mercury with respect to the Sun ($\mathbf{r}_{\mathrm{M}\odot} = \mathbf{r}_{\mathrm{M}} - \mathbf{r}_{\odot}$) changes as follows:

$$\begin{aligned}\mathbf{r}_{\mathrm{M}\odot}^{SEP} &= \mathbf{r}_{\mathrm{M}} - \mathbf{r}_{\odot}^{SEP} \\ &= \mathbf{r}_{\mathrm{M}} - \left(\mathbf{r}_{\odot} + \Delta\mathbf{r}_{\odot}^{SEP}\right) \\ &= \mathbf{r}_{\mathrm{M}\odot} - \Delta\mathbf{r}_{\odot}^{SEP}\end{aligned} \tag{A.19}$$

The correction on the point-mass acceleration of Mercury with respect to the Sun is calculated by taking the central gravity acceleration with the SEP corrected relative position and subtracting the conventional central gravity solution:

$$\begin{aligned}\mathbf{a}_{\mathrm{M}\odot}^{SEP} &= \left(\mathbf{a}_{\mathrm{M}\odot}^{CG}\right)_{\eta\neq 0} - \left(\mathbf{a}_{\mathrm{M}\odot}^{CG}\right)_{\eta=0} \\ &= -\frac{\mu_{\odot}}{\left(r_{\mathrm{M}\odot}^{SEP}\right)^3}\mathbf{r}_{\mathrm{M}\odot}^{SEP} + \frac{\mu_{\odot}}{r_{\mathrm{M}\odot}^3}\mathbf{r}_{\mathrm{M}\odot} \\ &= -\frac{\mu_{\odot}}{\left(r_{\mathrm{M}\odot} - \Delta r_{\odot}^{SEP}\right)^3}\left(\mathbf{r}_{\mathrm{M}\odot} - \Delta\mathbf{r}_{\odot}^{SEP}\right) + \frac{\mu_{\odot}}{r_{\mathrm{M}\odot}^3}\mathbf{r}_{\mathrm{M}\odot}\end{aligned} \tag{A.20}$$

Using the following relation A.21:

$$\frac{\partial r^n}{\partial \mathbf{r}} = n \cdot r^{n-2} \cdot \mathbf{r}^T \tag{A.21}$$

the partial derivatives of the acceleration correction with respect to position are described as:

$$\begin{aligned}\frac{\partial \mathbf{a}_{\mathrm{M}\odot}^{SEP}}{\partial \mathbf{r}_{\mathrm{M}\odot}} &= \mu_\odot \left[\frac{\partial}{\partial \mathbf{r}_{\mathrm{M}\odot}} \left(-\frac{1}{\left(r_{\mathrm{M}\odot} - \Delta r_\odot^{SEP}\right)^3} \left(\mathbf{r}_{\mathrm{M}\odot} - \Delta \mathbf{r}_\odot^{SEP}\right) \right) + \frac{\partial}{\partial \mathbf{r}_{\mathrm{M}\odot}} \left(\frac{1}{r_{\mathrm{M}\odot}^3} \mathbf{r}_{\mathrm{M}\odot} \right) \right] \\ &= \mu_\odot \left[-\frac{1}{\left(r_{\mathrm{M}\odot} - \Delta r_\odot^{SEP}\right)^3} \mathbf{I} + 3 \left(\mathbf{r}_{\mathrm{M}\odot} - \Delta \mathbf{r}_\odot^{SEP}\right) \frac{\left(\mathbf{r}_{\mathrm{M}\odot} - \Delta \mathbf{r}_\odot^{SEP}\right)^T}{\left(r_{\mathrm{M}\odot} - \Delta r_\odot^{SEP}\right)^5} + \frac{1}{r_{\mathrm{M}\odot}^3} \mathbf{I} - 3 \mathbf{r}_{\mathrm{M}\odot} \frac{\mathbf{r}_{\mathrm{M}\odot}^T}{r_{\mathrm{M}\odot}^5} \right]\end{aligned} \tag{A.22}$$

Finally, the partial derivative with respect to η can be found by taking $\Delta \mathbf{r}_\odot^{SEP} = \eta \cdot \mathbf{d}$ in equation A.20, which then gives:

$$\frac{\partial \mathbf{a}_{\mathrm{M}\odot}^{SEP}}{\partial \eta} = \frac{3\mu_\odot \mathbf{d} \left[\left(\mathbf{r}_{\mathrm{M}\odot} - \eta \mathbf{d}\right) \cdot \left(\mathbf{r}_{\mathrm{M}\odot} - \eta \mathbf{d}\right) \right]}{\left(r_{\mathrm{M}\odot} - \eta d\right)^5} - \frac{\mu_\odot \mathbf{d}}{\left(r_{\mathrm{M}\odot} - \eta d\right)^3} \tag{A.23}$$

After the acceleration models are implemented, the Nordtvedt equation (eq. A.14) needs to be implemented in the estimation model. It is not mentioned in any other publications with similar experiments how exactly this linear relation between estimatable parameters is taken care of in the estimation, so there are unfortunately no other examples to build on. Two approaches have been tested when developing our estimation algorithm:

1. Do not estimate η, but calculate it using the Nordtvedt equation when fetching the acceleration due to a SEP violation. The formal error is calculated by applying the following property of the variance of a linear equation:

$$\mathrm{Var}\left(\sum_{i=1}^{m} a_i X_i \right) = \sum_{i=1}^{m} \sum_{j=1}^{n} a_i a_j \, \mathrm{Cov}\left(X_i, X_j\right) \tag{A.24}$$

   The formal variance of η can be calculated by applying this property to the Nordtvedt constraint:

$$\begin{aligned}\mathrm{Var}\left(\eta\right) = \mathrm{Var}\left(\gamma\right) + 16\mathrm{Var}\left(\beta\right) + \mathrm{Var}\left(\alpha_1\right) + \frac{4}{9}\mathrm{Var}\left(\alpha_2\right) - 8\mathrm{Cov}\left(\gamma, \beta\right) \\ + 2\mathrm{Cov}\left(\gamma, \alpha_1\right) + \frac{4}{3}\mathrm{Cov}\left(\gamma, \alpha_2\right) - 8\mathrm{Cov}\left(\beta, \alpha_1\right) - \frac{16}{3}\mathrm{Cov}\left(\beta, \alpha_2\right) + \frac{4}{3}\mathrm{Cov}\left(\alpha_1, \alpha_2\right)\end{aligned} \tag{A.25}$$

   This approach is straightforward and easily verified, a disadvantage is that apriori information of the uncertainty of η cannot be used as additional information in the estimation.

2. Estimate η and enforce the linear relation between estimatable parameter using a constrained least-squares estimation algorithm (exact implementation is taken from [7, ch. 16]). This approach punishes the parameters from drifting off the solution of the Nordtvedt equation by increasing the residual. With this method the Nordtvedt equation is not strictly true after the estimation is done because the least-squares method is linearised, but within the formal uncertainties of all parameters the solution should be found. The approach of adding the Nordtvedt equation as a constraint is also used in some form in [39], although the estimation methods are very different form ours.

The second approach could not be validated, its results contained high true to formal error ratio's for β and η due to a high correlation between the two. After many attempts to fix this the second approach was dropped, because the first method did pass validation and therefore it is adopted in our work.

A consequence of the first approach is that η is not estimated and therefore equation A.23 is not used, but the SEP violation correction does become a function of PPN parameters γ, β, α_1 and α_2, as η can be expressed as a function of them. Using a chain rule, the following partial derivatives are implemented:

$$\frac{\partial \mathbf{a}_{\mathrm{M}\odot}^{SEP}}{\partial \gamma} = -\frac{\partial \mathbf{a}_{\mathrm{M}\odot}^{SEP}}{\partial \eta} \qquad \frac{\partial \mathbf{a}_{\mathrm{M}\odot}^{SEP}}{\partial \beta} = 4\frac{\partial \mathbf{a}_{\mathrm{M}\odot}^{SEP}}{\partial \eta} \tag{A.26}$$

$$\frac{\partial \mathbf{a}_{\mathrm{M}\odot}^{SEP}}{\partial \alpha_1} = -\frac{\partial \mathbf{a}_{\mathrm{M}\odot}^{SEP}}{\partial \eta} \qquad \frac{\partial \mathbf{a}_{\mathrm{M}\odot}^{SEP}}{\partial \alpha_2} = -\frac{2}{3}\frac{\partial \mathbf{a}_{\mathrm{M}\odot}^{SEP}}{\partial \eta} \tag{A.27}$$

A.4. Relativistic correction due to PPN parameters α_1 and α_2

PPN parameters α_1 and α_2 are present in the Nordtvedt equation (see equation A.14). Many metric theories of gravity assume α_1 and α_2 to be equal to zero, including General Relativity. However, they are not experimentally constrained to such a level that they can be neglected compared to γ and β. Therefore, if η is estimated, α_1 and α_2 are included in the estimation alongside. This is also done in more recent publications about estimations done with BepiColombo tracking, for example [49] and [27].

In the relativistic equations of motion, α_1 and α_2 show up in the first-order Schwarzschild relativistic term. Currently, in TUDAT the calculation of the Schwarzschild term is taken as a two-body acceleration from [44, eq. 10.12] and only includes γ and β. For a body B accelerating body A:

$$\mathbf{a}_{\mathrm{S},\gamma\beta} = \frac{GM_B}{c^2 r^3}\left\{\left[2(\beta+\gamma)\frac{GM_B}{r} - \gamma(\mathbf{v}\cdot\mathbf{v})\right]\mathbf{r} + \left[2(1+\gamma)\right](\mathbf{r}\cdot\mathbf{v})\mathbf{v}\right\} \tag{A.28}$$

This two-body acceleration is also given by [55, eq. 7.42] in a more general form, where the PPN parameters besides γ and β are included in the derivation, which is adopted for this work. For our implementation $M_B >> M_A$ and therefore the simplification is made that $M_A + M_B \approx M_B$. The complete Schwarzschild correction including all PPN parameters is then defined as follows:

$$\begin{aligned}\mathbf{a}_{\mathrm{S}} = \frac{GM_B}{c^2 r^3}\Bigg\{\Bigg[&2(\beta+\gamma)\frac{GM_B}{r} - \gamma(\mathbf{v}\cdot\mathbf{v}) + (2+\alpha_1-2\zeta_2)\frac{GM_A}{r} \\ &- \frac{1}{2}(6+\alpha_1+\alpha_2+\alpha_3)\frac{M_A}{M_B}(\mathbf{v}\cdot\mathbf{v}) + \frac{3}{2}(1+\alpha_2)\frac{M_A}{M_B}\left(\mathbf{v}\cdot\frac{\mathbf{r}}{r}\right)^2\Bigg]\mathbf{r} \\ &+ \left[2(1+\gamma) - \frac{M_A}{M_B}(2-\alpha_1+\alpha_2)\right](\mathbf{r}\cdot\mathbf{v})\mathbf{v}\Bigg\}\end{aligned} \tag{A.29}$$

PPN parameters α_3 and ζ_2 are neglected (see section A.6), and the correction can be slightly simplified:

$$\begin{aligned}\mathbf{a}_{\mathrm{S}} = \frac{GM_B}{c^2 r^3}\Bigg\{\Bigg[&2(\beta+\gamma)\frac{GM_B}{r} - \gamma(\mathbf{v}\cdot\mathbf{v}) + (2+\alpha_1)\frac{GM_A}{r} \\ &- \frac{1}{2}(6+\alpha_1+\alpha_2)\frac{M_A}{M_B}(\mathbf{v}\cdot\mathbf{v}) + \frac{3}{2}(1+\alpha_2)\frac{M_A}{M_B}\left(\mathbf{v}\cdot\frac{\mathbf{r}}{r}\right)^2\Bigg]\mathbf{r} \\ &+ \left[2(1+\gamma) - \frac{M_A}{M_B}(2-\alpha_1+\alpha_2)\right](\mathbf{r}\cdot\mathbf{v})\mathbf{v}\Bigg\}\end{aligned} \tag{A.30}$$

For convenience of analysing the impact of α_1 and α_2 in the propagation and estimation, the terms that are not considered in TUDAT by default are modelled as a separate correction alongside equation A.28, which takes the form:

$$\begin{aligned}\mathbf{a}_{\mathrm{S},\alpha_1\alpha_2} = \frac{GM_B}{c^2 r^3}\Bigg\{\Bigg[&(2+\alpha_1)\frac{GM_A}{r} - \frac{1}{2}(6+\alpha_1+\alpha_2)\frac{M_A}{M_B}(\mathbf{v}\cdot\mathbf{v}) + \frac{3}{2}(1+\alpha_2)\frac{M_A}{M_B}\left(\mathbf{v}\cdot\frac{\mathbf{r}}{r}\right)^2\Bigg]\mathbf{r} \\ &- \frac{M_A}{M_B}(2-\alpha_1+\alpha_2)(\mathbf{r}\cdot\mathbf{v})\mathbf{v}\Bigg\}\end{aligned} \tag{A.31}$$

For the estimation, the following partial derivatives are derived, which are very similar to the partial derivatives for the correction in equation A.28 as already implemented in TUDAT. The partial derivative with respect to position:

$$\begin{aligned}\frac{\partial \mathbf{a}_{\mathrm{S},\alpha_1\alpha_2}}{\partial \mathbf{r}} = \frac{GM_B}{c^2 r^3}\Bigg\{&(2+\alpha_1)\frac{GM_A}{r}\left[\mathbf{I} - \frac{\mathbf{r}\cdot\mathbf{r}^T}{r^2}\right] - \frac{1}{2}(6+\alpha_1+\alpha_2)\frac{M_A}{M_B}(\mathbf{v}\cdot\mathbf{v})\cdot\mathbf{I} \\ &+ \frac{3}{2}(1+\alpha_2)\frac{M_A}{M_B}\frac{(\mathbf{v}\cdot\mathbf{r})}{r^2}\left[2\cdot\mathbf{r}\cdot\mathbf{v}^T - \frac{2(\mathbf{v}\cdot\mathbf{r})}{r^2}\cdot\mathbf{r}\cdot\mathbf{r}^T + (\mathbf{v}\cdot\mathbf{r})\cdot\mathbf{I}\right] \\ &- \frac{M_A}{M_B}(2-\alpha_1+\alpha_2)(\mathbf{v}\cdot\mathbf{v}^T)\Bigg\} - 3\frac{\mathbf{a}_{\mathrm{SS},\alpha_1\alpha_2}\cdot\mathbf{r}^T}{r^2}\end{aligned} \tag{A.32}$$

The partial derivative with respect to velocity:

$$\frac{\partial \mathbf{a}_{S,\alpha_1\alpha_2}}{\partial \mathbf{v}} = \frac{GM_A}{c^2 r^3}\left\{ -(6+\alpha_1+\alpha_2)(\mathbf{r}\cdot\mathbf{v}^T) + \frac{3(1+\alpha_2)}{r^2}(\mathbf{v}\cdot\mathbf{r})\cdot\mathbf{r}\cdot\mathbf{r}^T \right. \\ \left. -(2-\alpha_1+\alpha_2)\left(\mathbf{r}\cdot\mathbf{v}\cdot\mathbf{I}+\mathbf{v}\cdot\mathbf{r}^T\right)\right\} \tag{A.33}$$

The partial derivative with respect to gravitational parameter of the accelerating body GM_B:

$$\frac{\partial \mathbf{a}_{S,\alpha_1\alpha_2}}{\partial GM_B} = \frac{1}{c^2 r^3}\left\{\left[(2+\alpha_1)\frac{GM_A}{r} - \frac{1}{2}(6+\alpha_1+\alpha_2)\frac{M_A}{M_B}(\mathbf{v}\cdot\mathbf{v}) + \frac{3}{2}(1+\alpha_2)\frac{M_A}{M_B}\left(\frac{\mathbf{v}\cdot\mathbf{r}}{r}\right)^2\right]\mathbf{r} \right. \\ \left. -\frac{M_A}{M_B}(2-\alpha_1+\alpha_2)(\mathbf{r}\cdot\mathbf{v})\mathbf{v}\right\} \tag{A.34}$$

The partial derivative with respect to α_1:

$$\frac{\partial \mathbf{a}_{S,\alpha_1\alpha_2}}{\partial \alpha_1} = \frac{GM_B}{c^2 r^3}\left\{\left[\frac{GM_A}{r} - \frac{1}{2}\frac{M_A}{M_B}(\mathbf{v}\cdot\mathbf{v})\right]\mathbf{r} + \frac{M_A}{M_B}(\mathbf{r}\cdot\mathbf{v})\mathbf{v}\right\} \tag{A.35}$$

The partial derivative with respect to α_2:

$$\frac{\partial \mathbf{a}_{S,\alpha_1\alpha_2}}{\partial \alpha_2} = \frac{GM_A}{c^2 r^3}\left\{\left[-\frac{1}{2}(\mathbf{v}\cdot\mathbf{v}) + \frac{3}{2}\left(\frac{\mathbf{v}\cdot\mathbf{r}}{r}\right)^2\right]\mathbf{r} - (\mathbf{r}\cdot\mathbf{v})\mathbf{v}\right\} \tag{A.36}$$

A.5. Time variable gravitational moments

The aim of this thesis project is to investigate the influence of time variable gravitational moments. To implement this effect, a small addition is made to the spherical harmonics library of TUDAT. Following literature which indicates that the oblateness varies in a sinusoidal pattern (e.g. [3, 28, 58]), a correction on the spherical harmonics coefficients with degree d and order 0 is modelled with a sine around the mean value of the coefficient J_d. The correction c_{J_d} that will be added is expressed as follows:

$$c_{J_d}(t) = A\sin\left(\frac{2\pi}{P}t + \varphi\right) \tag{A.37}$$

The coefficient which will then be used for the spherical harmonics acceleration at a certain time t is then:

$$J_{d,\text{corrected}}(t) = J_d + c_{J_d}(t) \tag{A.38}$$

Three parameters are used to manipulate the correction. The period P and phase φ are configured such that the correction is in sync with the solar cycle: a period of 11 years with the phase set such that a minimum occurs at the 15$^{\text{th}}$ of December 2008[1]. The amplitude A will be implemented as an estimatable parameter in the least-squares estimation. For the implementation, the partial derivative of the spherical harmonics acceleration with respect to the A has to be included. Use will be made of the fact that the partial derivative with respect to the coefficient itself is already implemented in TUDAT. A simple chain rule gives the following partial derivative:

$$\frac{\partial \mathbf{a}_{\text{SH}}}{\partial A} = \frac{\partial \mathbf{a}_{\text{SH}}}{\partial J_d}\frac{\partial J_d}{\partial A} = \frac{\partial \mathbf{a}_{\text{SH}}}{\partial J_d}\sin\left(\frac{2\pi}{P}t + \varphi\right) \tag{A.39}$$

A.6. Excluded accelerations

A key point of this work is to critically look at all effects that could influence the orbit of Mercury and ignore no acceleration that could have an effect that is noticeable in the estimation (i.e. causes a position change higher than the observational noise level, approximately 30cm). Many effects were analysed prior to setting up the simulation, also ones that are not included in similar studies, for example effects caused by gravitational theories other than GR.

In the following list, effects that were considered but not included will be mentioned with a brief description. For additional information on the effects and their impact the reader is referred to the mentioned references.

[1] Solar cycle data taken from `http://sidc.oma.be/silso/`

- It is chosen to ignore PPN parameters $\alpha_3, \zeta_1, \zeta_2, \zeta_3, \zeta_4$ because they correspond to theories that violate the conservation of total momentum. Such theories are proposed but struggle to find experimental evidence, see [56, ch. 3] for a discussion. While it would be interesting to study exotic theories of gravity, including them would very likely require a lot of work and therefore it is outside of the scope of this thesis project.

  The consequence of this assumption is the following: parameters α_3 and ζ_2 show up in equation A.29, and therefore their presently known uncertainty could be considered. α_3 is constrained to a value of 0 with an uncertainty of 10^{-20} [56] and therefore can be safely neglected considering the uncertainty of the other PPN parameters. ζ_2 has constraints similar to γ and β, but its effect in equation A.29 is smaller, such that the results of our work will not change noticeably when it is considered.

- The central assumption of the PPN framework is that the Einstein Equivalence Principle (EEP) is true [30, 56]. One of the building blocks of the EEP is Local Lorentz Invariance (LLI), which states that "the output of any local non-gravitational experiment is independent of the freely-falling reference frame in which it is performed" [56]. While it is tested to be correct to an astonishing level of 10^{-22} [33], much attention is devoted to proving or disproving LLI from the field of particle physics, as it plays an important role in the search for quantum gravity [35].

  To quantify violations and describe their effects on gravitational interactions, the Standard Model Extension (SME) formalism was developed [5], which uses twenty coefficients to describe the effects that can be determined through experiments (for an extensive overview see [31, 35]). Also Solar System dynamics can be used to constrain the perturbations caused by SME coefficients. This is for example done in [25] by using supplementary advances of perihelia from INPOP10a [15]. The analysis benefits from a large variety of observations from many Solar System bodies. Better tracking data of Mercury will of course improve this data set (as explicitly mentioned in [25]), and even more valuable data will be the tracking of asteroids using GAIA [24]. However, is not expected that an independent experiment of Mercury is able to find competitive bounds, and therefore including SME coefficients is considered to be out of the scope of this work.

- It has been suggested that the gravitational pull of dark matter in the Solar System can provide a relevant perturbation on the planetary orbits. The density and distribution of dark matter in the Solar System is not measured, so the exact gravitational pull is unknown. An upper bound has been found by studying the perihelion precession of planets in ephemeris EPM2011 [47]. The upper limit is still orders of magnitude higher than the suggested density of dark matter in the Solar System [19], even for theories which suggest that dark matter clumps in the Solar System due to gravitational interactions [29, 57]. Especially Jupiter and Saturn are good candidates to study this perturbation as they have a larger mass of dark matter within their orbits, which is a leading factor in the perturbation. With a Mercury-based experiment it is not expected that gravitational interactions due to dark matter can be detected considering the current upper bound.

- Modified Newtonian Dynamics (MOND) [13, 40] is a theory of gravity formulated in an attempt to solve the missing mass problem in a variety of astronomical observations (dark matter is currently the most popular answer to this problem). MOND reformulates Newton's law of gravity such that on galactic scales the magnitude of the force is different. The most important consequence on Solar System dynamics is that the gravitational potential of the Milky Way can cause an additional perturbation (this is called the external field effect). The effect however increases with distance from the Sun and current upper bounds on this effect have been estimated with Cassini tracking data [23]. Therefore, similarly to the last bullet, it is not expected that this effect is detectable using Mercury as a test body.

- Effects on the propagation of radio signals, such as the relativistic delay and deflection of light [55, 56] the influence of solar or interplanetary plasma (e.g. [53]), or errors caused by the uncertainty in the Earth's ephemeris or ground station locations are not taken into account in any way. The observational accuracy of MESSENGER and BepiColombo tracking data is directly adopted from literature (which will be elaborated in section B.1) under the assumption that in the calculation of the noise level all relevant effects on the transmission of electromagnetic signals are considered.

B

Observation construction

All observational data is simulated using the built-in capabilities of TUDAT. An observational error has to be simulated as well, which should be as close as possible to the real situation as encountered in the mission. In this appendix, an explanation will be given how the observations and errors are simulated.

The basis of the observation construction is given by the geometry between Earth, Mercury and a Mercury orbiter of which a schematic drawing is given in figure B.1. The position of planet Mercury over time with respect to Earth ($r_{\mathrm{E-M}}$) is what is of interest for the experiments on gravity such as the one in this report, but this vector cannot be directly determined using spacecraft data. Range measurements between the spacecraft with respect to Earth ($r_{\mathrm{E-S/C}}$) is what is provided in the spacecraft tracking data, as well as range-rate (Doppler) measurements. The position of the orbiter with respect to Mercury ($r_{\mathrm{S/C-M}}$) can be determined through orbit determination.

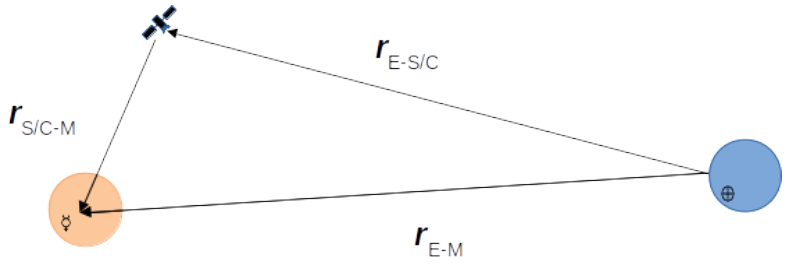

Figure B.1: Schematic overview of the geometry between Earth, Mercury an orbiter around Mercury

The standard in the field is to perform simultaneous numerical integration of planet Mercury and its orbiter, and subsequently determine the orbit of the spacecraft around Mercury and the orbit of Mercury around the Solar System Barycentre (SSB) in one estimation (e.g. [21] for MESSENGER and [27, 49] for Bepi-Colombo). Because of the short orbital period of the spacecraft around Mercury, the integration step size has to be small for such a simultaneous integration (in the order of 1 minute), while for Mercury around the SSB it can be much larger (in the order of hours). On an average laptop it is unfeasible to perform such an integration for a period of 20 years, both in terms of processing speed and RAM. Therefore, in this project, the simplification is made to only numerically integrate planet Mercury.

The consequence of this simplification is that the spacecraft is taken out of the equation entirely. The range observations are simulated to be between the Earth and the centre of gravity of Mercury ($r_{\mathrm{E-M}}$). When simply changing the source of the range tracking data to the centre of gravity of Mercury, the errors introduced by the orbit determination of the spacecraft with respect to Mercury are ignored. To compensate, an analysis was performed of what the errors typically are of the spacecraft with respect to Mercury, with the goal of artificially adding to the simulated observations of the centre of gravity of Mercury to mimic the errors encountered in the real process.

This process wil be explained in a few steps. First, in section B.1, a brief overview is given of the characteristics of the tracking data, and the variables used in this work. In section B.2, the method and results of this analysis is explained. In section B.3 it is explained how observation errors are simulated in the gravity experiment.

B.1. MESSENGER and BepiColombo tracking characteristics

For the missions, all relevant parameters to describe the tracking is taken from literature and presented in table B.1.

Table B.1: Characteristics of the tracking data of MESSENGER and BepiColombo

	MESSENGER	BepiColombo
Mercury flyby's during cruise	14/1/2008 6/10/2008 29/9/2009	1/10/2021 23/6/2022 20/6/2023 5/9/2024 2/12/2024 9/1/2015
tracking arc duration per day	6 h [36]	8 h (Ka only) [8]
tracking start	1/4/2011	1/4/2026
tracking end	1/3/2015	1/4/2018
maximum number of tracking days	900 [21]	-
two-way range accuracy	0.5 - 3.0 m [21]	0.3 m [49]
range measurement frequency	300 s [21]	300 s [49]
two-way range-rate accuracy	0.1 mm/s [36]	0.003 mm/s [49]
range-rate integration time	60 s [36]	1000 s [49]

A few notes concerning these tracking settings:

- For the range accuracy of the MESSENGER tracking system, the Sun-Probe-Earth (SPE) angle plays an important role. The accuracy gets worse the closer the path of the signal comes to the Sun. For the range measurements the error level is at its minimum of 0.5 meters at SPE angle of 180 degrees and at its maximum of 3 meters at SPE angle of 35 degrees [36]. For the error construction in our simulations, the angle is calculated at each step and the error level is determined based on a linear trend between these two extremes. For SPE angles lower than 35 degrees, range errors rise drastically [36] and are not considered useful anymore [21, 43]. The MORE instrument does not suffer from this error increase at low SPE angle due to its multi-frequency tracking capabilities, and therefore its range error is constant.
- For BepiColombo, data is transmitted in both Ka-band and X-band frequencies, and received by two ground stations for a total of 15 hours per day. However, only one has Ka-band downlink capabilities which receives data for 8 hours each day [8]. The X-band data has an error ten times larger for both the range and range-rate measurements [49]. Because the value of X-band tracking data is much less in this work but does mean twice the processing power, X-band tracking data is ignored.
- Even though over 1000 tracking days are identified for MESSENGER, it was identified by [21] that a maximum of 900 tracking tracking days are useful due to spacecraft operations or anomalies on other days. This will be adopted in our simulation, and tracking days are taken out at random to end up with a maximum of 900 days.

B.2. Orbiter error with respect to Mercury

To analyse what the orbit determination errors of the spacecraft around Mercury are, several spacecraft tracking arcs are simulated along the lifetime of each mission. In these arcs, the spacecraft is numerically integrated around Mercury. The spacecraft initial state and the every state of Mercury are taken from SPICE kernels. Subsequently it is attempted to estimate the initial state of the spacecraft to get an idea of the position error of the spacecraft with respect to Mercury.

The orbit determination of the spacecraft during these arcs is done in a least-squares estimation. As observations, simulated range-rate tracking data is used. In the gravity experiment only simulated two-way range data will be used and range-rate data will be ignored. This decoupling of the tracking data is not unusual for orbit determination and navigation of interplanetary missions [52]. In the simultaneous estimation, range-rate data will provide the most important information of the spacecraft relative to the planet, while the range between Earth and the spacecraft will not change considerably over one spacecraft orbit but will change considerably over one Mercury orbit around the Sun [21]. Therefore it is not expected that much quality will

be lost by doing the two estimations separately with separate data products instead of estimating simultaneously.

For each mission 24 arcs were simulated, spaced evenly between the start and end date. In addition to the state of the spacecraft, also the largest sources of perturbations on the trajectory are included in the numerical integration of the spacecraft in each arc: the perturbations by the planets, the spherical harmonic gravity field of Mercury up to degree and order 8 and the solar radiation pressure. The initial states of all arcs are then estimated using a least-squares estimation. Gravity field coefficients $C_{n,m}$ and the radiation pressure coefficient are also included in the parameter estimation.

After the formal errors of the initial states are determined, the errors are propagated along the arc by using the state transition matrix in order to get the error at each point in time for the error, which is the goal of this analysis. An example of the result for one arc and the maximum error for all arcs are seen in respectively the left and right side of figure B.2. All errors are given in a Mercury-centric reference frame. When studying the results was discovered that there are two types of modulation in the formal error level of state coordinates:

- A modulation that is visible within one tracking arc, with the period of the orbit of the spacecraft around Mercury. The errors are smallest when the spacecraft is at its perihermion. As output of the analysis, for every arc a table is made what the average error is at a certain true anomaly.
- When comparing the maximum errors, the behaviour seems somewhat random. It is however expected that this is caused by the geometry of the spacecraft around Mercury, and Mercury and Earth around the Sun. This effect is e.g. also be seen in [2, 21]. The exact period of this variation is hard to determine due to the low number of samples, but it is clear that the accuracy of the orbit determination varies along the mission duration.

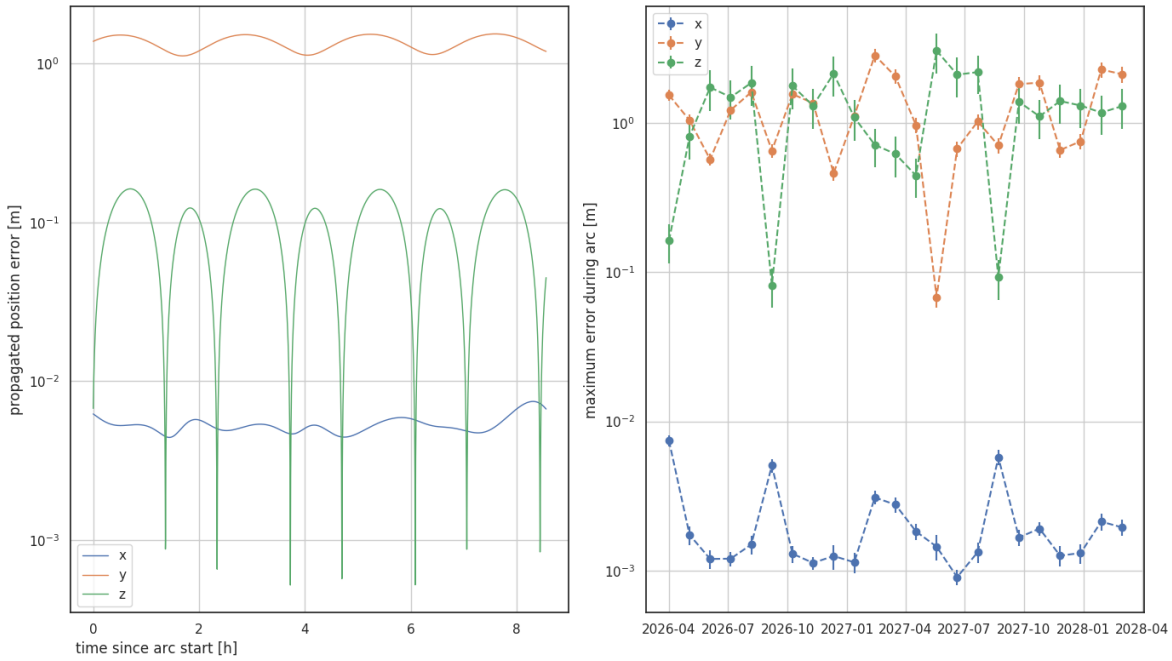

Figure B.2: The results of the orbit determination of BepiColombo for selected tracking arcs. On the left, propagated spacecraft position errors during one BepiColombo tracking arc. On the right, the maximum error of each of the 24 simulated BepiColombo arcs during the mission duration.

This information will help to achieve the goal of getting an estimate of the spacecraft orbit determination errors to simulate our observations. Unfortunately the simulated arcs only cover a small portion of the total mission duration, and in between the arcs the spacecraft errors are unknown. The following algorithm is set up to get an estimate for each coordinate at a given in time:

1. Through SPICE it is retrieved what the true anomaly of the spacecraft is at the input time.

2. For the arc before and after the input time, it is retrieved what the typical error level is at the retrieved true anomaly from the tabulated data mentioned above.

3. By setting a linear interpolator using the two times of the arcs as independent variables and the error levels as dependent value, the error level at the input time is calculated.

B.3. Simulated error construction

In the situation presented in figure B.1, the vector from Earth to Mercury $r_{\text{E-M}}$ is constructed through simple geometry:

$$r_{\text{E-M}} = r_{\text{E-S/C}} + r_{\text{S/C-M}} \tag{B.1}$$

The range measurements are simulated using the built-int capabilities of TUDAT and are provided as a distance d (one-dimensional). Using the tools presented so far in this appendix, an error sample for each observation is generated in the following way:

1. The typical error level of the range measurement from an Earth ground station to the spacecraft $\sigma_{d_{\text{E-S/C}}}$ is calculated according to the information given in section B.1.

2. The typical error level of the spacecraft with respect to Mercury is determined according to the information given in section B.2. The error is determined in three dimensions: $\sigma_{x_{\text{S/C-M}}}$, $\sigma_{y_{\text{S/C-M}}}$, $\sigma_{z_{\text{S/C-M}}}$. This three-dimensional error is projected onto the unit vector of $r_{\text{E-M}}$ to retrieve the typical error on the range measurement due to the orbit determination of the spacecraft around Mercury: $\sigma_{d_{\text{S/C-M}}}$.

3. The typical error level of the range between Earth and Mercury is then achieved by taking the root mean square of these two error levels:
$$\sigma^2_{d_{\text{E-M}}} = \sigma^2_{d_{\text{E-S/C}}} + \sigma^2_{d_{\text{S/C-M}}}$$

4. Using a normal distribution with mean 0 and standard deviation $\sigma^2_{d_{\text{E-M}}}$, a random sample is generated for the noise error.

The knowledge of the typical error level at certain points in time can also be used help the estimation algorithm in the gravity experiment, by using observation weighting matrix $\mathbf{W}$ in the least-squares calculation. This approach is also done in reality because it is usually known what the relative quality between observations is (depending on e.g. SPE, true anomaly). The weight of each observation is calculated as $1/\sigma^2_{d_{\text{E-M}}}$.

B.4. Validity of simulated errors

The formal errors of the initial states of the arcs are in the order of 10-100 meters for MESSENGER and in the order of 0.1-1 metres BepiColombo. Only a few examples could be found of what typical errors are for the initial states in reality (or in the case of BepiColombo, expectations):

- [21, 54] show range residuals for MESSENGER in the order of meters to hundreds of meters, but the error levels are very dependent on the Mercury ephemeris used.

- [54] shows that the state of MESSENGER has 1σ errors of up to 30 meters for each state, which matches well with our estimates.

- [2] expects errors in the initial condition of BepiColombo tracking arcs in the order of 0.1-1 meters.

Roughly our errors seem to be equal or a bit higher than encountered in the examples that could be found. Therefore the errors used in the gravity experiment are assumed to be slightly on the conservative side.

A critical note should be added based on the fact that for different arcs along the mission lifetime, the state errors look different (the second type of modulation that was mentioned in section B.2). Because of computational limits only a limited amount of arcs could be simulated, and therefore it is unknown what exactly the period of this modulation is because of a scarce number of samples. Therefore interpolation had to be used, and it can be expected that at certain times in the missions the error samples can be incorrect. The important result of the simulation of various arcs along the missions, is to get an idea of what typical errors along the missions lifetime are: with 20+ arcs it is assumed that the maximum and minimum errors

that are encountered during the missions are captured. To conclude, while at specific points in time it is not expected that the error samples are spot on compared to reality, this method does provide a distribution of errors along the mission of which we can be confident that they occur in reality.

To judge whether our simplifications lead to observation errors as close to the real situation as possible, most of all the validation procedures were used as explained in appendix D. In spite of the simplifications, the reproduction of the results in the papers is successful, and therefore it is concluded that this approach does not introduce any problems of considerable size in this research.

C

Verification

C.1. Numerical integrator and propagator

In this study, the orbit of Mercury is numerically integrated from the time of the first MESSENGER flyby (January 2008) until the final day of the nominal BepiColombo mission (March 2027). In this time span of almost 20 years, the accuracy of the position of Mercury is expected play a role in the order of centimetres. The BepiColombo range measurements have an uncertainty of 30 centimetres [49]. If the estimation performs as desired, it is expected that Mercury's position coordinates can be estimated to this level. Therefore, a suitable numerical integrator and propagator should be chosen that ideally has a numerical error that is low with respect to these values.

In addition, it should be taken into account that the correction of the position of the Sun due to a violation of the Strong Equivalence Principle (section A.3) is in the order of a centimetres for a typical value of $|\eta| \approx 10^{-5}$. If this correction in position of the Sun is in the order of the numerical error, it will become impossible to estimate η correctly.

To test the numerical integration of Mercury's orbit, as a first step different numerical integrators with different step sizes have been tested. All possible accelerations (relativistic effects, dynamic $J_{2\odot}$ and $J_{4\odot}$) are included such that the complexity of the acceleration model is at the maximum that will be encountered in this study. As numerical propagators the following options were considered:

- Runge-Kutta 4 (RK4), a multi-stage integrator which is known less suitable for orbital mechanics due to the linearisation that is performed, but is included to provide a reference for the other integrators.
- Runge-Kutta-Fehlberg 7(8) (RK78), a multi-stage integrator which is a straightforward integrator and known to work well for a wide range of orbital dynamics [41].
- Adam-Bashford Moulton of order 8 and 12 (ABM8, ABM12), two multi-step integrators which are often used in numerical integration of Solar System bodies for generating planetary ephemerides [14, 42].

the RK7(8) and ABM integrators provide the option to implement variable step size and variable order. This is especially beneficial for eccentric orbits, but the integrator is more complex and harder to control and understand. With the eccentricity of Mercury's orbit being 0.21, perhaps the step size could be relatively larger at its aphelion with respect to its perihelion and some computation time can be saved, but the difference is not expected to be large. To simplify the choice for an integrator, only constant step sizes and orders are considered in this work.

This analysis was first performed with double precision (15 digits) for the state of Mercury, which turned out to be insufficient: the numerical rounding errors that occurred early in the integration were propagated over 20 years, causing the minimum error at the end to be in the order of 1 meter. For integration results accurate to centimetres, additional precision was required. It was chosen to integrate the orbit with long double precision (18 digits), of which the results are presented in this section.

The integration was performed for a range of step sizes from a maximum of 12 hours to a minimum of 5 minutes (which is when the limit is hit in terms of RAM). After the integration is done, the orbits are also integrated backwards, and the maximum error between the forward integration and backward integration

is computed. The results can be seen on the left of figure C.1. Because RK7(8) is a multi-stage method, more function evaluations are needed per step compared to the other integrators. To make a fair comparison of performance vs computational effort, the maximum errors are plotted against the number of function evaluations in the right of figure C.1.

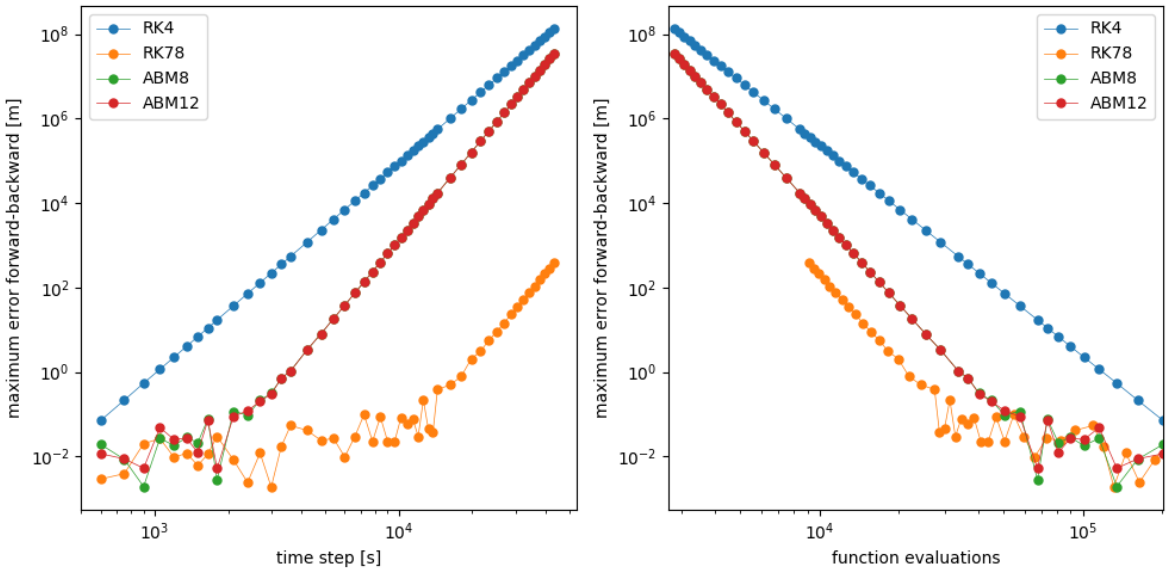

Figure C.1: Comparison of integrators: maximum error after subtracting results from forward integration minus backward integration, plotted against the time step (left) and function evaluations (right)

At high step sizes, the truncation error is dominant, indicated by the linear part of the plot. For each integrator except RK4, the numerical limit is reached, as can be seen in the erratic behaviour for low step sizes. While the last digit in Mercury's coordinates around the Solar System Barycentre is in the order of 10^{-8} meters, the integration duration of 20 years causes the numerical rounding errors to propagate to maximum values that are just around or below the centimetre level. This comes very close to our requirements. Therefore, optimising for computational effort is seen as less of a priority and the integrator with the best performance is chosen, which is the RK7(8) integrator with a step size of 3000 seconds. The maximum error between forward and backward integration is 1.87 millimetres.

In an attempt to decrease errors by numerical integration even further, the different propagators that are implemented in Tudat are compared. In the development of the simulation the Cowell propagator was used, which is the default in Tudat and also used in the analysis in the previous section. However, the orbit of Mercury in this thesis can be characterised by a distinct two-body problem between the Sun and Mercury ($O(10^{-2})$ m/s), and many perturbations by planets ($\leq O(10^{-7})$ m/s), relativistic effects ($\leq O(10^{-9})$ m/s)) and the zonal spherical harmonics of the Sun ($\leq O(10^{-12})$ m/s). Therefore, a propagator that models the orbit as a two-body problem with perturbations can be expected to yield better result compared to the Cowell integrator.

In this section, the Cowell integrator is compared with the other options in TUDAT that use 6 parameters to describe the state[1]: Encke, Gauss-Keplerian and Gauss-Modified-Equinoctial. For the integrator, the result of the previous section is used: RK7(8) with a step size of 3000 seconds. Similarly to previous section, the integration is also performed backwards and the forward and backward integration are compared.

Because the integrator is already in the regime of numerical rounding errors, the propagator analysis was ran twice (once the initial state was slightly perturbed) to see if behavior of a propagator was not based purely on rounding luck. The results of the two runs can be seen in figures C.2 and C.3.

[1] `https://tudat.tudelft.nl/tutorials/tudatFeatures/propagationSetup/propagatorSettingsCoordinates.html#tudatfeaturespropagatorsettingscoordinates`

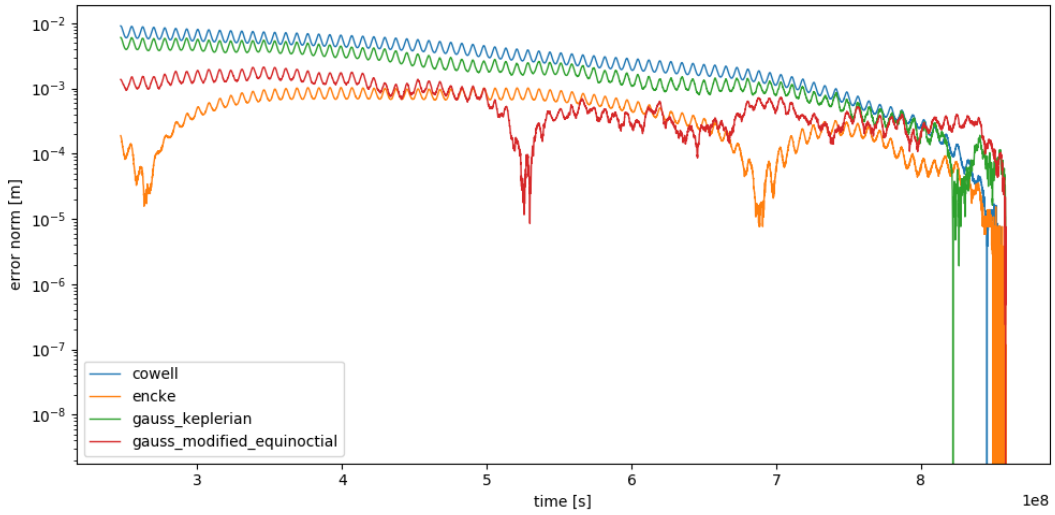

Figure C.2: Comparison of propagators: maximum error after subtracting results from forward integration minus backward integration

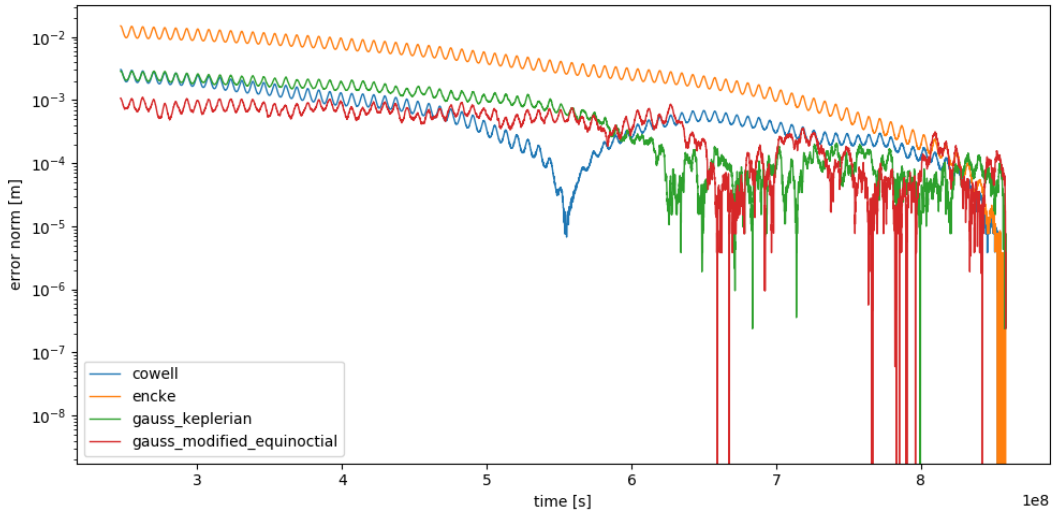

Figure C.3: Comparison of propagators: maximum error after subtracting results from forward integration minus backward integration, after the initial state was slightly perturbed

It is noticed between the two figures that the Encke propagator is especially unpredictable: once being the best propagator and once being the worst. For this reason it is not considered a responsible choice. The other choices all have a maximum error below 1 centimetre and are considered suitable. To maximise performance, the Gauss-modified-equinoctial is chosen, as the increase in error over time seems the least compared to the other two (outside of the regime of numerical rounding errors).

For the final choice for integrator and propagator, the forward minus backward error is compared with the SEP violation correction of the position of the Sun. Both quantities are plotted for each of the position coordinates in figure C.4 for a typical run of the parameter estimation, were a relatively small value was obtained for a typical N7ordtvedt parameter $\eta = 5 \cdot 10^{-6}$ (formal errors are usually in the range $10^{-5} - 10^{-6}$). While the magnitude of the SEP correction is close to the numerical error level, the behaviour is very different (short period versus long period), and therefore it is expected that the estimation algorithm will be able to properly separate these two effects.

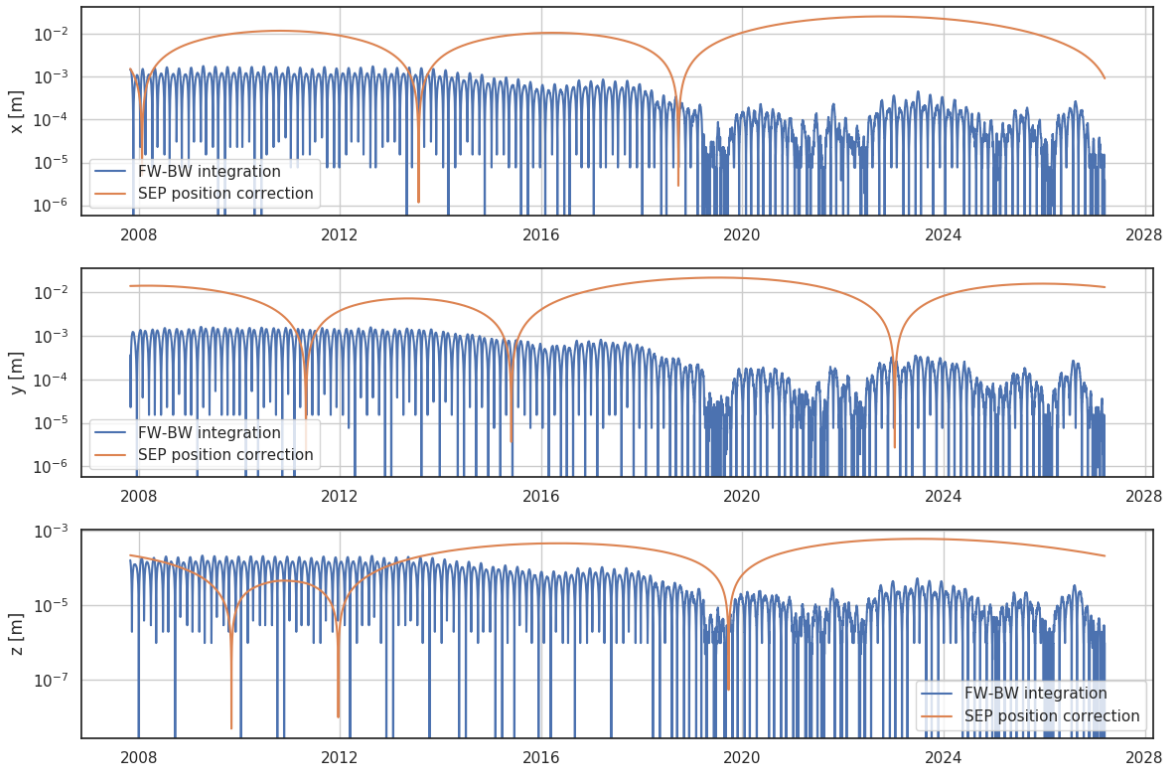

Figure C.4: Forward minus backward propagation (blue) versus SEP violation correction of the Sun (orange)

C.2. Acceleration partial derivatives

For the acceleration partial derivatives given in appendix A, unit tests have been written to verify the derivation and implementation. Each acceleration partial is calculated with a central difference scheme, and the result compared to the result of the derived partial derivative. The relative difference between each entry of the partial derivative is calculated, and the partial derivatives were verified to be accurate until the relative tolerances reported in table C.1.

Table C.1: Relative tolerances for which the acceleration partial matches with a central difference calculation.

Acceleration	w.r.t. state	w.r.t. parameters
Schwarzschild	10^{-4}	10^{-4}
Lense-Thirring	10^{-5}	10^{-4}
SEP Violation	10^{-6}	10^{-5}
Time varying gravitational parameter	10^{-5}	10^{-5}
Spherical harmonics w.r.t. $J_{2\odot}$ amplitude	-	10^{-5}

Considering that the partial derivatives will be used in a least-squares algorithm where a linearised approach is used, which is an approximation by definition, these partial derivatives are assumed to be sufficiently accurate. Any errors that could be caused by slight offsets in the partial derivatives can be handled by iteration in the estimation.

After this verification was done and results were generated, large true errors appeared of a factor 200 higher than the formal errors in the estimation of the amplitude of the $J_{2\odot}$ correction. Residuals of 1 order of magnitude higher than the noise level were the result for the BepiColombo range measurements. Such results are usually an indication that some kind of numerical integration errors cause high true errors in the parameter estimation. Because the problem only occurred when including the amplitude in the estimation it was also suspected that the partial derivative with respect to the amplitude had something to do with it, perhaps it was not correctly derived or implemented. However, after long and careful investigation, it could not be found what the source was of this error. This section verifies that the partial derivative is derived and

implemented correctly, and the previous section verifies that numerical errors are far below the BepiColombo noise levels.

Because it was suspected that the source of the error was numerical errors, it was attempted to perform the integration backwards. In this way, the numerical errors for the final years during the BepiColombo mission should be smaller, and due to propagation numerical errors should be largest at the beginning of the MESSENGER mission. It was hoped that this method would prevent high numerical errors during the final year which has the most accurate observations, while relatively higher numerical errors in the MESSENGER phase might not matter as much because the observation errors are also higher.

Because the source of the problem could not be found, the backward-integration approach seemed to provide a great work-around for the high true to false error ratio problem. The results for an estimation where forward and backward integration were used are compared in table C.2. The estimation results with a backward integration look successful and also the residuals were at the expected noise level.

Table C.2: Results of the parameter estimation when the state of Mercury is integrated forwards and backwards, when including amplitude $A_{J_{2\odot}}$ of the solar oblateness in the estimation.

		γ	β	η	$J_{2\odot}$	$\frac{G\dot{m}_\odot}{Gm_\odot}\,[\mathrm{y}^{-1}]$	$A_{J_{2\odot}}$
forward integration	true errors	$2.4\cdot10^{-6}$	$3.4\cdot10^{-6}$	$1.1\cdot10^{-5}$	$1.5\cdot10^{-10}$	$4.2\cdot10^{-15}$	$5.9\cdot10^{-9}$
	formal errors	$1.8\cdot10^{-6}$	$7.5\cdot10^{-7}$	$4.7\cdot10^{-6}$	$3.7\cdot10^{-10}$	$1.3\cdot10^{-15}$	$2.6\cdot10^{-11}$
	t/f error ratio	1.3	4.5	2.4	0.4	3.3	227.3
backward integration	true errors	$3.6\cdot10^{-7}$	$1.7\cdot10^{-6}$	$7.0\cdot10^{-6}$	$3.3\cdot10^{-10}$	$2.1\cdot10^{-15}$	$1.4\cdot10^{-11}$
	formal errors	$1.8\cdot10^{-6}$	$7.5\cdot10^{-7}$	$4.7\cdot10^{-6}$	$3.7\cdot10^{-10}$	$1.3\cdot10^{-15}$	$2.6\cdot10^{-11}$
	t/f error ratio	0.2	2.2	1.5	0.9	1.7	0.55

While integration backwards in time might not be intuitive, it does not matter which way the integration is performed for the parameter estimation. Only the result of the integration is used: the state of Mercury at certain points in time. Therefore by using this method no side effects are expected. To verify, a test is performed with the estimation without the amplitude, which does not suffer from the numerical error problem that is spoken of in this section. Results when using forward and backward integration are compared in table C.3, the formal are equal in both cases.

Table C.3: Results of the parameter estimation when the state of Mercury is integrated forwards and backwards, not including the amplitude $A_{J_{2\odot}}$ of the solar oblateness in the estimation.

		γ	β	η	$J_{2\odot}$	$\frac{G\dot{m}_\odot}{Gm_\odot}\,[\mathrm{y}^{-1}]$
forward integration	true errors	$6.6\cdot10^{-6}$	$2.3\cdot10^{-6}$	$2.4\cdot10^{-6}$	$1.3\cdot10^{-9}$	$1.6\cdot10^{-16}$
	formal errors	$1.8\cdot10^{-6}$	$7.5\cdot10^{-7}$	$4.7\cdot10^{-6}$	$3.7\cdot10^{-10}$	$4.9\cdot10^{-16}$
	t/f error ratio	3.7	3.0	0.5	3.5	0.3
backward integration	true errors	$7.0\cdot10^{-6}$	$1.4\cdot10^{-6}$	$1.4\cdot10^{-6}$	$1.4\cdot10^{-9}$	$2.1\cdot10^{-15}$
	formal errors	$1.8\cdot10^{-6}$	$7.5\cdot10^{-7}$	$4.7\cdot10^{-6}$	$3.7\cdot10^{-10}$	$4.9\cdot10^{-16}$
	t/f error ratio	3.8	1.8	0.3	3.7	4.3

Note: results in tables C.2 and C.3 are better than those in the journal article because results are shown without consider covariance added. This is because the formal errors increase after adding consider covariance, after which a comparison between true and formal error is no longer representative for having a good or bad estimation result..

C.3. Consider Covariance

The goal of the consider covariance analysis is to consider the uncertainty of certain parameters without having to actually include them in the estimation. To verify the implementation of the consider covariance analysis, a comparison is made between including a parameter as an estimated parameter and a consider parameter. Specifically, it is desired to know if the consider covariance addition to covariance matrix $\boldsymbol{P}$, as given by equation C.1 [41], is the same as the uncertainty increase that would be seen when including the parameter in the estimation.

$$\boldsymbol{P}^c = \boldsymbol{P} + \left(\boldsymbol{P}\boldsymbol{H}_x^T\boldsymbol{W}\right)\left(\boldsymbol{H}_c\boldsymbol{C}\boldsymbol{H}_c^T\right)\left(\boldsymbol{P}\boldsymbol{H}_x^T\boldsymbol{W}\right)^T \tag{C.1}$$

As a case study, the angular momentum $\boldsymbol{S}_\odot$ of the Sun is taken, one of the consider parameters that will be used in this study. The value of $190 \cdot 10^{39}$ kgm^{2}s^{-1} and an apriori uncertainty of $1.5 \cdot 10^{39}$ kgm^{2}s^{-1} is used in all simulations performed, which come from [45]. For an estimation of parameters using the MESSENGER mission, the resulting formal errors are given in table C.4 for when $\boldsymbol{S}_\odot$ is estimated (column 1) and when it is not estimated (column 2). The difference between the two is given (column 3), and finally the consider covariance addition, the second term in equation C.1 (column 4).

Table C.4: verification of formal errors when using the Solar angular momentum as consider parameter

	$\boldsymbol{S}_\odot$ estimated	$\boldsymbol{S}_\odot$ not estimated	difference	consider covariance
x [m]	0.446	0.446	$1.572 \cdot 10^{-7}$	$1.568 \cdot 10^{-7}$
y [m]	0.451	0.451	$4.148 \cdot 10^{-8}$	$4.150 \cdot 10^{-8}$
z [m]	0.718	0.718	$1.670 \cdot 10^{-5}$	$1.670 \cdot 10^{-5}$
V_x [m/s]	$3.05 \cdot 10^{-7}$	$3.05 \cdot 10^{-7}$	$6.912 \cdot 10^{-13}$	$6.912 \cdot 10^{-13}$
V_y [m/s]	$3.28 \cdot 10^{-7}$	$3.28 \cdot 10^{-7}$	$1.045 \cdot 10^{-12}$	$1.045 \cdot 10^{-12}$
V_z [m/s]	$5.85 \cdot 10^{-7}$	$5.85 \cdot 10^{-7}$	$8.474 \cdot 10^{-11}$	$8.476 \cdot 10^{-11}$
γ [-]	$1.63 \cdot 10^{-5}$	$1.63 \cdot 10^{-5}$	$1.273 \cdot 10^{-9}$	$1.273 \cdot 10^{-9}$
β [-]	$3.53 \cdot 10^{-5}$	$3.53 \cdot 10^{-5}$	$4.571 \cdot 10^{-9}$	$4.572 \cdot 10^{-9}$
η [-]	$3.00 \cdot 10^{-4}$	$3.00 \cdot 10^{-4}$	$2.076 \cdot 10^{-15}$	$2.094 \cdot 10^{-15}$
$\dot{\mu_\odot}/\mu_\odot$ [y^{-1}]	$1.73 \cdot 10^{-14}$	$1.73 \cdot 10^{-14}$	$9.345 \cdot 10^{-21}$	$9.373 \cdot 10^{-21}$
$\mu_\odot$ [m^{3}s^{-2}]	$1.36 \cdot 10^{8}$	$1.36 \cdot 10^{8}$	$1.064 \cdot 10^{2}$	$1.065 \cdot 10^{2}$
$J_{2\odot}$ [-]	$1.27 \cdot 10^{-9}$	$1.27 \cdot 10^{-9}$	$1.146 \cdot 10^{-14}$	$1.146 \cdot 10^{-14}$
$\boldsymbol{S}$ [kgm^{2}s^{-1}]	$1.50 \cdot 10^{39}$	-	-	-

The formal errors of both estimations are very similar, indicating that the influence of $\boldsymbol{S}_\odot$ on the estimation is not very significant. The estimation is also not able to find an improvement for the uncertainty on $\boldsymbol{S}_\odot$. The difference between the two estimations matches very well with the consider covariance addition to the formal errors. This verifies the consider covariance approach.

The consider covariance analysis has been attempted for a number of other parameters as well, yielding the same results. It should be noted that once an improvement can be found in the formal error of a parameter with respect to its apriori uncertainty, the covariance of this parameter and other parameters goes down as well, resulting in lower errors for all parameters (except when correlation is zero). For this reason, including something as a consider parameter instead of estimatable parameter can harm the results across the board. This finding has been taken into careful consideration when selecting the consider parameters as mentioned in section 2.3 of the journal article (chapter 2).

D

Validation

To validate the simulation and estimation in TUDAT, it is attempted to reproduce papers that use either MESSENGER or BepiColombo (simulated) tracking data to estimate relativistic parameters. The strategy is to try to set up the simulation and estimation as close as possible to how it is done by other authors, and get out the same results, validating that our software is at least as good as the software used in peer-reviewed journal papers.

First, let us set some expectations for this strategy. Setting up a simulation and estimation requires many design choices, and usually very few choices are disclosed in the journal articles where the results are presented. For BepiColombo, many simulations of experiments similar to this thesis work have already been performed. Even though they all try to simulate exact same physical experiment, results can be far apart. As an example various results for the formal error of PPN parameter β, one of the main goals of such publications, is shown in table D.1. Most of all this is indicative that the results of such an experiment should be taken with a grain of salt, and that in our results and discussion the exact numbers of an outcome should not be used for detailed discussion, but rather the order of magnitude of the results or relative results. Besides, because the implementation in the TUDAT software as well as custom made additions for this thesis work will differ from the methods used in the other publications, the validation cannot be expected to be entirely accurate. If any formal errors can be reproduced within a factor two, we will already consider it a good result.

Table D.1: Formal errors of PPN parameter β from publications that simulated an experiment using BepiColombo tracking data.

publication	formal error on β
Milani et al. 2002 [39]	$7.6 \cdot 10^{-5}$
Ashby et al. 2007 [4]	$5.7 \cdot 10^{-4}$
Iess et al. 2009 [26]	$2.5 \cdot 10^{-6}$
Schettino et al. 2015 [49]	$3.8 \cdot 10^{-7}$
Schettino et al. 2016 [50]	$6.7 \cdot 10^{-7}$
Imperi et al. 2018 [27]	$1.0 \cdot 10^{-6}$

The choices for papers to reproduce is based on the considerations above: those are used that disclose as much as possible about their setup, such that the reproduction can be done as close as possible to the original. For MESSENGER, the paper of Antonio Genova et al. in 2018 is used [21], as the methods are very well explained in the paper, some of the derived acceleration models are even adopted in this work. It is expected that the reproduction is able to match very well with the original if done correctly. For BepiColombo, a source where the methods are explained in such detail is unfortunately not available. Two papers are chosen which are the best candidates: by Giulia Schettino et al. in 2015 [49] and by Luigi Imperi et al. in 2018 [27].

The next sections present the results for each of the papers. The results and comparisons with the paper are given in tables. The meaning of each column is clarified below:

- parameter: the parameter for which the results are given. "η (nv-eq)" indicates that the Nordtvedt parameter and its errors are calculated through the Nordtvedt equation (eq. A.14), which is the case if the Nordtvedt equation is assumed to be true.

- apriori σ: the apriori value that is used as input for the estimation.
- true σ: the true error of the estimated parameter.
- formal σ: the formal error of the estimated parameter, calculated with the covariance matrix P that is output of the least-squares estimation.
- t/f ratio: ratio between absolute true error (column 3) and formal error (column 4). For a successful estimation this ratio should be around or lower than 1.
- f/a improv.: ratio between the apriori error (column 2) and the formal error (column 4), i.e. how much the uncertainty on the parameter has improved with respect to the apriori value.
- paper formal σ: the formal error of the estimated parameter that is reported in the publication.
- f/p ratio: the ratio between the formal error of our estimation (column 4) and the formal error reported in the publication (column 7). The aim of this validation is to get this ratio as close to 1 as possible, which is an indicator that the papers results can be perfectly reproduced.

D.1. Genova et al. 2018

This publication tries to estimate various relativity parameters using the MESSENGER tracking data set. Many acceleration models described in this paper have been adopted in this work (see appendix A). Because the acceleration models are the same for both simulations, trying to reproduce this paper is a reliable indicator if our script is able to simulate the MESSENGER tracking data and its errors well. It is also the only comparison made in this chapter where the results are based on actual data (as BepiColombo is still cruising towards Mercury).

Some noteworthy settings of estimation described by the paper:

- The Nordtvedt equation is assumed to be true.
- γ is implemented as a consider parameter, therefore it is not included in the estimation results.
- PPN parameters α_1 and α_2 are neglected in this paper.

The results of the reproduction can be seen in table D.2.

Table D.2: Validation results of the reproduction of Genova et al. 2018 [21].

parameter	apriori σ	true σ	formal σ	t/f ratio	f/a improv.	paper formal σ	f/p ratio
β	6.90e-05	9.28e-06	2.02e-05	0.70	3.41	1.80e-05	1.125
$\dot{\mu_\odot}/\mu_\odot$	2.90e-14	6.65e-14	2.12e-14	3.13	1.37	1.47e-14	1.444
$\mu_\odot$	1.40e+08	-1.34e+09	1.37e+08	9.93	1.03	3.50e+08	0.390
$J_{2\odot}$	3.00e-09	-1.90e-09	3.43e-09	0.95	0.88	2.00e-09	1.714
η (nv-eq)	3.00e-04	3.71e-05	8.42e-05	0.64	3.56	7.20e-05	1.169

The ratio's between the papers results and our results match very well, better than initially expected, and it can definitely concluced that the validation is succesful. One stands out: the gravitational parameter of the Sun. In the paper, the formal uncertainty of $\mu_\odot$ increases with respect to the apriori information. The apriori uncertainty of the gravitational parameter of the Sun is taken from INPOP13c [16], an ephemeris, and apparently the MESSENGER data alone is not enough to improve the uncertainty. In our simulation this is also the case as portrayed by the relatively high true error. It however seems to be a characteristic of TUDAT that the formal error does not go higher than the apriori level but as a maximum stays on the same level. This causes the difference in the comparison with the paper in the last column.

D.2. Schettino 2015

This publication is a full-cycle simulation of BepiColombo tracking data, and the estimation of parameters that can be done with it. While the effects that are taken into account are described, their explicit implementation is not named, and therefore it is not possible to know what assumptions and approximations were made when constructing the acceleration model. Therefore it can be expected that there are some differences between the models which could affect the validation results.

Some noteworthy settings of estimation described by the paper:

- The Nordtvedt equation is assumed to be true.
- It is assumed that during the BepiColombo cruise phase, an improvement for γ can be found in a superior solar conjunction experiment. The current precision of γ is also based on such an experiment with the Cassini spacecraft [6]. The assumed result of γ from the experiment for BepiColombo are taken as apriori uncertainty.
- PPN parameters α_1 and α_2 are estimated, however it is not disclosed if they are only used in the Nordtvedt equation or also play a role in the acceleration model. The latter is true in our acceleration model (see section A.4).
- Flyby's during the cruise phase are not included in the tracking data.

The results of the validation can be seen in table D.3.

Table D.3: Validation results of the reproduction of Schettino et al. 2015 [49].

parameter	apriori σ	true σ	formal σ	t/f ratio	f/a improv.	paper formal σ	f/p ratio
γ	2.00e-06	7.13e-06	1.95e-06	3.66	1.03	8.90e-07	2.191
β	1.10e-04	1.84e-04	1.26e-06	145.70	87.23	3.80e-07	3.319
α_1	4.00e-06	7.26e-04	3.99e-06	181.68	1.00	4.80e-07	8.321
α_2	8.00e-10	-2.85e-11	8.00e-10	0.04	1.00	6.90e-08	0.012
$\dot{\mu_\odot}/\mu_\odot$	4.10e-14	3.30e-14	1.42e-14	2.33	2.89	2.00e-14	0.708
$\mu_\odot$	1.40e+08	8.47e+08	5.75e+07	14.73	2.43	4.00e+07	1.437
$J_{2\odot}$	3.00e-09	-1.91e-08	3.95e-10	48.46	7.59	3.70e-10	1.068
η (nv-eq)	4.50e-04	2.22e-06	2.00e-06	1.11	224.98	2.00e-06	1.000

Unlike the paper, no improvements could be found for the uncertainties of PPN parameters α_1 and α_2. The cause for this difference between the paper and our results is unclear. Instead, high true errors are present in the results of our simulation with respect to the formal errors . This disturbs the estimation of all parameters, and while the results in the last columns match well except for α_1 and α_2, the high true to formal error ratio means the result cannot be trusted. As no improvements could be found for α_1 and α_2, perhaps the consider covariance analysis could provide an alternative. The results of this adjusted approach can be seen in table D.4.

Table D.4: Validation results of the reproduction of Schettino et al. 2015 [49], with PPN parameters α_1 and α_2 as consider parameters.

parameter	apriori σ	true σ	formal σ	t/f ratio	f/a improv.	paper formal σ	f/p ratio
γ	2.00e-06	5.93e-06	1.95e-06	3.04	1.03	8.90e-07	2.191
β	1.10e-04	1.17e-06	7.69e-07	1.52	143.13	3.80e-07	2.023
$\dot{\mu_\odot}/\mu_\odot$	4.10e-14	9.10e-15	1.42e-14	0.64	2.89	2.00e-14	0.708
$\mu_\odot$	1.40e+08	1.35e+08	5.74e+07	2.35	2.44	4.00e+07	1.436
$J_{2\odot}$	3.00e-09	1.15e-09	3.79e-10	3.04	7.91	3.70e-10	1.025
η (nv-eq)	4.50e-04	-1.25e-06	4.47e-06	0.28	100.62	2.00e-06	2.236

In these results the high true to formal error ratios are gone, and the ratios in the final column also match well. The fact that we take into account the uncertainties of α_1 and α_2 but do not estimate them seems to allow the other parameters to be estimated very well in comparison to the paper. It is a pity that improvements on α_1 and α_2 cannot be reported in this work, but as the focus of the research question lies mainly on β and $J_{2\odot}$, it is seen as a valid approach for our purposes.

D.3. Imperi 2018

For the BepiColombo mission, it is attempted to reproduce a second paper. This publication is a full simulation of BepiColombo tracking data, and the writers simulate all the experiments that can be performed with it, one of which is the estimation of relativity parameters.

Some noteworthy settings of estimation described by the paper:

- Two configurations are tested: one where the Nordtvedt equation is true, and one where the Nordtvedt equation is false.
- Again, it is assumed that during the BepiColombo cruise phase, an improvement for γ can be found in a superior solar conjunction experiment. The current precision of γ is also based on such an experiment with the Cassini spacecraft [6]. The assumed result of γ from the experiment for BepiColombo are taken as apriori uncertainty.
- PPN parameters α_1 and α_2 are estimated, and they show up in the acceleration model [27, eq. 1] similar to ours but instead expressed in orbital elements (see section A.4), (it is shown that they are the same in [55, sec. 7.3].
- It is uncertain whether flyby's are included in the tracking data. It is assumed no flyby's are included (it has been tested with flyby's, the difference is minimal anyway)

The results are given when the Nordtvedt equation is set to true in table D.5 and false in D.6.

Table D.5: Validation results of the reproduction of Imperi et al. 2018 [27], Nordtvedt equation set to be true.

parameter	apriori σ	true σ	formal σ	t/f ratio	f/a improv.	paper formal σ	f/p ratio
γ	1.10e-06	-4.38e-05	1.10e-06	39.91	1.00	1.10e-06	0.999
β	3.90e-05	-1.10e-02	1.24e-06	8863.28	31.37	1.00e-06	1.243
α_1	4.00e-06	-4.42e-02	4.00e-06	11051.41	1.00	6.10e-07	6.553
α_2	8.00e-10	1.74e-09	8.00e-10	2.17	1.00	1.30e-07	0.006
$\dot{\mu_\odot}/\mu_\odot$	4.30e-14	2.02e-13	4.65e-15	43.34	9.25	2.80e-14	0.166
$\mu_\odot$	1.00e+10	-3.79e+10	2.92e+07	1298.79	342.66	5.30e+07	0.551
$J_{2\odot}$	9.00e-09	1.24e-06	2.65e-10	4662.96	33.98	5.50e-10	0.482
η (nv-eq)	4.50e-04	1.39e-04	2.67e-06	52.08	168.83	3.00e-06	0.888

Table D.6: Validation results of the reproduction of Imperi et al. 2018 [27], Nordtvedt equation set to be false.

parameter	apriori σ	true σ	formal σ	t/f ratio	f/a improv.	paper formal σ	f/p ratio
γ	1.10e-06	0.00e+00	1.10e-06	0.00	1.00	1.10e-06	0.999
β	3.90e-05	0.00e+00	2.64e-05	0.00	1.48	2.80e-05	0.942
η	4.50e-04	1.00e-10	2.69e-06	0.00	166.99	3.30e-06	0.817
α_1	4.00e-06	-2.22e-01	4.00e-06	55387.28	1.00	6.60e-07	6.061
α_2	8.00e-10	8.68e-09	8.00e-10	10.85	1.00	1.30e-07	0.006
$\dot{\mu_\odot}/\mu_\odot$	4.30e-14	0.00e+00	4.67e-15	0.00	9.20	2.80e-14	0.167
$\mu_\odot$	1.00e+10	0.00e+00	9.44e+07	0.00	105.89	9.90e+07	0.954
$J_{2\odot}$	9.00e-09	0.00e+00	2.98e-09	0.00	3.02	3.20e-09	0.932

A very similar conclusion can be drawn compared to last section. Even with the acceleration model being similar in terms of effects caused by α_1 and α_2, the same problem as the previous section occurs, meaning it is not a problem related to a specific paper. Again, because no improvement can be found, implementing α_1 and α_2 as consider parameters could be a better approach. The results are given when the Nordtvedt equation is set to true in table D.7 and false in D.8. Again, this approach seems to work very well and will be adopted to generate results.

Table D.7: Validation results of the reproduction of Imperi et al. 2018 [27], Nordtvedt equation set to be true, with PPN parameters α_1 and α_2 as consider parameters.

parameter	apriori σ	true σ	formal σ	t/f ratio	f/a improv.	paper formal σ	f/p ratio
γ	1.10e-06	1.40e-06	1.10e-06	1.28	1.00	1.10e-06	0.999
β	3.90e-05	1.93e-07	7.45e-07	0.26	52.33	1.00e-06	0.745
$\dot{\mu_\odot}/\mu_\odot$	4.30e-14	3.36e-14	2.30e-14	1.46	1.87	2.80e-14	0.823
$\mu_\odot$	1.00e+10	1.72e+08	8.91e+07	1.93	112.26	5.30e+07	1.681
$J_{2\odot}$	9.00e-09	3.37e-10	2.45e-10	1.38	36.80	5.50e-10	0.445
η (nv-eq)	4.50e-04	-6.31e-07	4.81e-06	0.13	93.58	3.00e-06	1.603

Table D.8: Validation results of the reproduction of Imperi et al. 2018 [27], Nordtvedt equation set to be false, with PPN parameters α_1 and α_2 as consider parameters.

parameter	apriori σ	true σ	formal σ	t/f ratio	f/a improv.	paper formal σ	f/p ratio
γ	1.10e-06	2.71e-07	1.10e-06	0.25	1.00	1.10e-06	0.999
β	3.90e-05	-1.50e-04	2.74e-05	5.47	1.42	2.80e-05	0.980
η	4.50e-04	-1.88e-06	2.70e-06	0.70	166.41	3.30e-06	0.819
$\dot{\mu_\odot}/\mu_\odot$	4.30e-14	2.55e-14	2.34e-14	1.09	1.84	2.80e-14	0.836
$\mu_\odot$	1.00e+10	-4.18e+08	1.20e+08	3.49	83.49	9.90e+07	1.210
$J_{2\odot}$	9.00e-09	1.74e-08	3.11e-09	5.60	2.89	3.20e-09	0.972

Bibliography

[1] A. Ajabshirizadeh et al. Contribution of the Solar Magnetic Field on Gravitational Moments. *Scientia Iranica*, 15(1), 2008.

[2] E.M. Alessi et al. Desaturation manoeuvres and precise orbit determinationfor the BepiColombo mission. *Monthly Notices of the Royal Astronomical Society*, 423(3):2270–2278, 2012.

[3] H.M. Antia et al. Temporal Variations in the Sun's Rotational Kinetic Energy. *Astronomy & Astrophysics*, 477(2), 2007.

[4] N. Ashby et al. Future gravitational physics tests from ranging to the BepiColombo Mercury planetary orbiter. *Physical Review D*, 75(2), 2007.

[5] Q.G. Bailey and V.A. Kostelecký. Signals for Lorentz violation in post-Newtonian gravity. *Physical Review D*, 74(4), 2006.

[6] B. Bertotti et al. A test of general relativity using radio links with the Cassini spacecraft. *Nature*, 425: 374–376, 2003.

[7] S. Boyd and L. Vandeberghe. *Introduction to Applied Linear Algebra*. Camebridge University Press, 2018.

[8] S. Cicalo et al. The BepiColombo MORE gravimetry and rotation experimentswith theORBIT14 software. *Monthly Notices of the Royal Astronomical Society*, 457(2), 2016.

[9] R.H. Dicke and H.M. Goldenberg. Solar Oblateness and General Relativity. *Physical Review Letters*, 18 (9), 1967.

[10] D. Dirkx et al. Propagation and estimation of the dynamical behaviour of gravitationally interacting rigid bodies. *Astrophysics and Space Science*, 364(37), 2019.

[11] A. Einstein. Zur Elektrodynamik bewegter Körper. *Annalen der Physik*, 332(10):891–921, 1905.

[12] A. Einstein. Die Grundlage der allgemeinen Relativitätstheorie. *Annalen der Physik*, 354(7):769–822, 1916.

[13] B. Famaey and S.S. McGaugh. Modified Newtonian Dynamics (MOND): Observational Phenomenology and Relativistic Extensions. *Living Reviews in Relativity*, 15(10), 2012.

[14] A. Fienga et al. INPOP06. A new numerical planetary ephemeris. *Astronomy and Astrophysics*, 477(1): 315–327, 2007.

[15] A. Fienga et al. The INPOP10a planetary ephemeris and its applications in fundamental physics. *Celestial Mechanics and Dynamical Astronomy*, 111:363–385, 2011.

[16] A. Fienga et al. Numerical estimation of the sensitivity of INPOP planetary ephemerides to general relativity parameters. *Celestial Mechanics and Dynamical Astronomy*, 123:325–349, 2015.

[17] A. Fienga et al. INPOP19a Planetary Ephemerides scientific notes. Technical report, Institute for Celestial Mechanics and Computation of Ephemerides, 2019.

[18] William M Folkner et al. The Planetary and Lunar Ephemerides DE430 and DE431. Technical report, Jet Propulsion Laboratory, 2014. IPN Progress Report 42-196.

[19] J.-M. Frère et al. Bound on the Dark Matter Density in the Solar System from Planetary Motions. *Physical Review Letters D*, 77(8), 2008.

[20] A. Genova et al. Mercury radio science experiment of the mission bepicolombo. *Memoire della Società Astronomica Italiana*, 75:282–286, 2008.

[21] A. Genova et al. Solar system expansion and strong equivalence principle as seen by the NASA MESSENGER mission. *Nature communications*, 9(289), 2018.

[22] D.H. Hathaway. The Solar Cycle. *Living Reviews in Solar Physics*, 12(4), 2015.

[23] A. Hees et al. Constraints on modified Newtonian dynamics theories from radio tracking data of the Cassini spacecraft. *Physical Review D*, 89(10), 2014.

[24] A. Hees et al. Tests of gravitation with Gaia observations of Solar System Objects, 2015. URL `https://arxiv.org/abs/1509.06868v2`.

[25] A. Hees et al. Testing Lorentz symmetry with planetary orbital dynamics. *Physical Review D*, 92(6), 2015.

[26] L. Iess et al. MORE: An advanced tracking experiment for the exploration of Mercury with the mission BepiColombo. *Acta Astronautica*, 65(5-6):666–675, 2009.

[27] L. Imperi et al. Ananalysis of the geodesy and relativity experiments of BepiColombo. *Icarus*, 301:9–25, 2018.

[28] A. Irbah et al. Variations of Solar Oblateness with the 22yr Magnetic Cycle Explain Apparently Inconsistent Measurements. *The Astrophysical Journal LEtters*, 875(2), 2019.

[29] I.B. Khriplovich and D.L. Shepelyansky. Capture of dark matter by the solar system. *International Journal of Modern Physics D*, 18(12), 2012.

[30] S.M. Kopeikin et al. *Relativistic Celestial Mechanics of the Solar System*. Wiley VCH, 2011.

[31] V.A. Kostelecký and N. Russel. Data Tables for Lorentz and CPT Violation. *Reviews of Modern Physics*, 83 (11), 2011. January 2019 update: `https://arxiv.org/abs/0801.0287v12`.

[32] J.R. Kuhn et al. The Precise Solar Shape and Its Variability. *Science*, 337(6102):1638–1640, 2012.

[33] S.K. Lamoreaux et al. New Limits on Spatial Anisotropy from Optically Pumped 201Hg and 199Hg. *Physical Review letters*, 57(25), 1986.

[34] U.J. Le Verrier. Theorie du mouvement de mercure. *Annales de l'Observatoire imperial de Paris*, 5, 1859.

[35] D. Mattingly. Modern tests of lorentz invariance. *Living Reviews in Relativity*, 8(5), 2005.

[36] E. Mazarico et al. The gravity field, orientation, and ephemeris of Mercury from MESSENGER observations after three years in orbit. *Journal of Geophysical Research: Planets*, 119(12), 2014.

[37] R. Mecheri et al. New values of gravitational moments J2 and J4 deduced from helioseismology. *Solar Physics*, 222(2), 2009.

[38] M. Meftah et al. On HMI solar oblateness during solar cycle 24 and impact of the space environment on results. *Advances in Space Research*, 58(7):1425–1440, 2016.

[39] A. Milani et al. Testing general relativity with the BepiColombo radio science experiment. *Physical Review D*, 66(8), 2002.

[40] M. Milgrom. A Modification of the Newtonian Dynamics as a Possible Alternative to the Hidden Mass Hypothesis. *The Astrophysical Journal*, 270:365–370, 1983.

[41] O. Montenbruck and E. Gill. *Satellite Orbits - Models, Methods and Applications*. Springer, 2000. Corrected 3rd printing 2005.

[42] X.X. Newhall. DE 102: a numerically integrated ephemeris of the Moon and planets spanning forty-four centuries. *Astonomy and Astrophysics*, 125(1):150–167, 1983.

[43] R.S. Park et al. Precession of Mercury's Perihelion from Ranging to the MESSENGER Spacecraft. *The Astronomical Journal*, 153(3), 2017.

[44] G. Petit and B. Luzum. *IERS Conventions*. Verlag des Bundesamts für Kartographie und Geodäsie, Frankfurt am Main, 2010. IERS Technical Note 36 Chapter 10.

[45] F.P. Pijpers. Helioseismic determination of the solar gravitational quadruple moment. *Monthly Notices of the Royal Astronomical Society*, 297:L76–L80, 1998.

[46] S. Pireaux and J.-P. Rozelot. Solar quadruple moment and purely relativistic gravitation contributions to Mercury's perihelion advance. *Astrophysics and Space Science*, 284(4):1159–1194, 2003.

[47] E.V. Pitjeva and N.P. Pitjev. Relativistic effects and dark matter in the solar system from observations of planets and spacecrafts. *Monthly Notices of the Royal Astronomical Society*, 432(4):3431–3437, 2013.

[48] J.-P. Rozelot and C Damiani. History of solar oblateness measurements and interpretation. *The European Physical Journal H*, 36(3):407–436, 2011.

[49] G. Schettino et al. The relativity experiment of MORE: Global full-cycle simulation and results. *2015 IEEE Metrology for Aerospace (MetroAeroSpace)*, pages 141–145, 2015.

[50] G. Schettino et al. Sensitivity study of systematic errors in the BepiColombo relativity experiment. In *2016 IEEE Metrology for Aerospace (MetroAeroSpace)*, pages 533–537, 2016.

[51] I.I. Shapiro. A century of relativity. *Reviews of Modern Physics*, 71(2), 1999.

[52] C.L. Thornton and J.S. Border. *Radiometric Tracking Techniques for Deep-Space Navigation*. Jet Propulsion Laboratory, California Institute of Technology, 2000. Monograph 1, Deep-Space Communications and Navigation Series.

[53] A.K. Verma et al. Electron density distribution and solar plasma correction of radio signals using MGS, MEX, and VEX spacecraft navigation data and its application to planetary ephemerides. *Astronomy & Astrophysics*, 550:A124, 2012.

[54] A.K. Verma et al. Use of messenger radioscience data to improve planetary ephemeris and to test general relativity. *Astronomy & Astrophysics*, 561(A115), 2014.

[55] C.M. Will. *Theory and Experiment in Gravitational Physics*. Cambridge University Press, 1981.

[56] C.M. Will. The Confrontation between General Relativity and Experiment. *Living Reviews in Relativity*, 17(4), 2014.

[57] X. Xu and E. R. Siegel. Dark matter in the solar system, 2008. URL `https://arxiv.org/abs/0806.3767`.

[58] Y. Xu et al. Perihelion precession caused by solar oblateness variation in equatorial and ecliptic coordinate systems. *Monthly Notices of the Royal Astronomical Society*, 472(3):2686–2693, 2017.